



Publication Year	2018
Acceptance in OA @INAF	2020-11-13T15:55:41Z
Title	Explorer of Enceladus and Titan (E2T): Investigating ocean worlds' evolution and habitability in the solar system
Authors	Mitri, Giuseppe; Postberg, Frank; Soderblom, Jason M.; Wurz, Peter; Tortora, Paolo; et al.
DOI	10.1016/j.pss.2017.11.001
Handle	http://hdl.handle.net/20.500.12386/28341
Journal	PLANETARY AND SPACE SCIENCE
Number	155

1 **Explorer of Enceladus and Titan (E²T): Investigating Ocean Worlds' Evolution and**
2 **Habitability in the Solar System**

3

4 Giuseppe Mitri ¹, Frank Postberg ², Jason M. Soderblom ³, Peter Wurz ⁴, Paolo Tortora ⁵, Bernd Abel
5 ⁶, Jason W. Barnes ⁷, Marco Berga ⁸, Nathalie Carrasco ⁹, Athena Coustenis ¹⁰, Jean Pierre Paul de
6 Vera ¹¹, Andrea D'Ottavio ⁸, Francesca Ferri ¹², Alexander G. Hayes ¹³, Paul O. Hayne ¹⁴, Jon K.
7 Hillier ¹⁵, Sascha Kempf ¹⁶, Jean-Pierre Lebreton ¹⁷, Ralph D. Lorenz ¹⁸, Andrea Martelli ⁸, Roberto
8 Orosei ¹⁹, Anastassios E. Petropoulos ¹⁴, Kim Reh ¹⁴, Juergen Schmidt ²⁰, Christophe Sotin ¹⁴, Ralf
9 Srama ²¹, Gabriel Tobie ¹, Audrey Vorburger ⁴, Véronique Vuitton ²², Andre Wong ¹⁴, Marco Zannoni

10 ⁵

11 ¹ LPG, Université de Nantes, France

12 ² University of Heidelberg, Germany

13 ³ Massachusetts Institute of Technology, USA

14 ⁴ University of Bern, Switzerland

15 ⁵ University of Bologna, Italy

16 ⁶ University of Leipzig, Germany

17 ⁷ University of Idaho, USA

18 ⁸ Thales Alenia Space, Italy

19 ⁹ LATMOS, France

20 ¹⁰ LESIA, Observ. Paris-Meudon, CNRS, Univ. P. et M. Curie, Univ. Paris-Diderot, France

21 ¹¹ DLR, Germany

22 ¹² University of Padova -CISAS, Italy

23 ¹³ Cornell University, USA

24 ¹⁴ Jet Propulsion Laboratory, California Institute of Technology, USA

25 ¹⁵ University of Kent, UK

26 ¹⁶ University of Colorado, USA

27 ¹⁷ LPC2E, France

28 ¹⁸ JHU Applied Physics Laboratory, USA

29 ¹⁹ INAF, Italy

30 ²⁰ University of Oulu, Finland

31 ²¹ University of Stuttgart, Germany

32 ²² Univ. Grenoble Alpes, CNRS, IPAG, France

33

34

April 29, 2017

35

36

Manuscript submitted to Planetary Space Science

37

38 **Corresponding Author:**

39

40 Giuseppe Mitri

41 Laboratoire de Planetologie et de Geodynamique

42 Université de Nantes

43 2 rue de la Houssinière

44 44322 Nantes, France

45 Giuseppe.Mitri@univ-nantes.fr

46 **Abstract**

47 Titan, with its organically rich and dynamic atmosphere and geology, and Enceladus, with its
48 active plume, both harbouring subsurface oceans, are prime environments in which to
49 investigate the habitability of ocean worlds and the conditions for the emergence of life. We
50 present a space mission concept, Explorer of Enceladus and Titan (E²T), dedicated to
51 investigating the evolution and habitability of these Saturnian satellites proposed as a
52 medium-class mission led by ESA in collaboration with NASA in response to ESA's M5
53 Cosmic Vision Call. E²T proposes a focused payload that would provide in-situ composition
54 investigations and high-resolution imaging during multiple flybys of Enceladus and Titan
55 using a solar-electric powered spacecraft in orbit around Saturn. The E²T mission would
56 provide high-resolution mass spectrometry of the plumes currently emanating from
57 Enceladus' south polar terrain and of Titan's changing upper atmosphere. In addition, high-
58 resolution infrared (IR) imaging would detail Titan's geomorphology at 50-100 m resolution
59 and the temperature of the fractures on Enceladus's south polar terrain at meter resolution.
60 These combined measurements of both Titan and Enceladus would enable the E²T mission
61 scenario to achieve two major scientific goals: 1) Study the origin and evolution of volatile-
62 rich ocean worlds; and 2) Explore the habitability and potential for life in ocean worlds. E²T's
63 two high-resolution time-of-flight mass spectrometers would enable to untangle the
64 ambiguities left by the NASA/ESA/ASI Cassini-Huygens mission regarding the identification
65 of low-mass organic species, detect high-mass organic species for the first time, further
66 constrain trace species such as the noble gases, and clarify the evolution of solid and volatile
67 species. The high-resolution IR camera would reveal the geology of Titan's surface and the
68 energy dissipated by Enceladus fractured south polar terrain and plume in detail unattainable
69 by the Cassini mission.

70

71 **1. Introduction**

72 The NASA/ESA/ASI Cassini-Huygens mission has revealed Titan and Enceladus to be two
73 unique worlds in the Solar System during its thirteen years of observations in the Saturnian
74 system (July 2004 - September 2017). Titan, with its organically rich and dynamic
75 atmosphere and geology, and Enceladus, with its active plume composed of multiple jets
76 (Waite et al., 2006; Spahn et al., 2006; Porco et al., 2006), both harbouring subsurface oceans
77 (Iess et al., 2010, 2012, 2014), are ideal environments in which to investigate the conditions
78 for the emergence of life and the habitability of ocean worlds as well as the origin and
79 evolution of complex planetary systems. The prime criteria of habitability include energy
80 sources, liquid water habitats, nutrients and a liquid transport cycle to move nutrients and
81 waste (McKay et al., 2008, 2016; Lammer et al., 2009). The best-known candidates in the
82 Solar System for habitability at present likely meeting these criteria are the ocean worlds in
83 the outer Solar System, which include: Europa, Enceladus, Ganymede and Titan (Lunine,
84 2016). While the Jovian moons will be thoroughly investigated by the ESA Jupiter Icy moon
85 Explorer (JUICE), Enceladus and Titan which provide environments that can be easily
86 sampled from orbit in a single mission, are not currently targeted by any future exploration.
87 The joint exploration of these two fascinating objects will allow us to better understand the
88 origin of their organic-rich environment and will give access to planetary processes that have
89 long been thought unique to the Earth.

90 Titan is an intriguing world similar to the Earth in many ways, with its dense nitrogen-
91 methane atmosphere and familiar geological features, including dunes, mountains, seas, lakes
92 and rivers (e.g., Stofan et al., 2007; Lorenz et al., 2009; Mitri et al., 2010). Titan undergoes
93 seasonal changes similar to Earth, driven by its orbital inclination of 27° and Saturn's
94 approximately 30 year orbit. Exploring Titan then offers the possibility to study physical

95 processes analogous to those shaping the Earth's landscape, where methane takes on water's
96 role of erosion and formation of a distinct geomorphological surface structure.

97 Enceladus is an enigma; it is a tiny moon (252 km radius) that harbours a subsurface
98 liquid-water ocean (Iess et al., 2014; McKinnon et al., 2015; Thomas et al., 2016), which jets
99 material into space. The eruption activity of Enceladus offers a unique possibility to sample
100 fresh material ejected from subsurface liquid water and understand how exchanges with the
101 interior controls surface activity as well as constrain the geochemistry and astrobiological
102 potential of internal oceans on ocean worlds (e.g., Porco et al., 2006). Since the 1997 launch
103 of the Cassini-Huygens mission, there has been great technological advancement in
104 instrumentation that would enable answering key questions that still remain about the
105 Saturnian ocean worlds.

106 We present a space mission concept, Explorer of Enceladus and Titan (E²T), dedicated to
107 investigating the evolution and habitability of Enceladus and Titan proposed as a medium-
108 class mission led by ESA in collaboration with NASA in response to ESA's M5 Cosmic
109 Vision Call. In Section 2 we present the science case for the future exploration of Enceladus
110 and Titan as proposed by the E²T mission, and Section 3 the science goals for the E²T
111 mission. In Sections 4 and 5 we discuss the proposed payload and mission and spacecraft
112 configuration necessary to achieve E²T mission goals.

113

114 **2. Science Case for the Exploration of Enceladus and Titan**

115 Titan, Saturn's largest satellite, is unique in the Solar System with its dense, extensive
116 atmosphere composed primarily of nitrogen (97%) and methane (1.4%) (e.g., Bézard, 2014),
117 and a long suite of organic compounds resulting from multifaceted photochemistry which
118 occurs in the upper atmosphere down to the surface (e.g., Israël et al., 2005; Waite et al.,
119 2007; Gudipati et al., 2013; Bézard, 2014). As methane is close to its triple point on Titan, it

120 gives rise to a methane cycle analogous to the terrestrial hydrological cycle, characterized by
121 cloud activity, precipitation, river networks, lakes and seas covering a large fraction of the
122 northern terrain (Figure 1) (e.g., Tomasko et al., 2005; Stofan et al., 2007; Mitri et al., 2007;
123 Hayes et al., 2008).

124 FIGURE 1

125 Titan's atmosphere shows many similarities with our own planet, but the low temperature
126 conditions and the absence of oxygen, render Titan a unique world to study on its own,
127 probably bringing essential information on the conditions prevailing on the primitive Earth.
128 The seasonal effects on Titan are essential to study. With an environment that changes on a
129 29.5 year cycle, it is crucial to study the satellite during an entire orbital period. Cassini has
130 investigated Titan over only two seasons: from Northern winter solstice to summer solstice.
131 And while ground-based observations, have observed Titan in other seasons, the data are not
132 sufficient to address many of the outstanding questions. Current measurements with
133 Cassini/CIRS show that the chemical content of Titan's atmosphere has significant seasonal
134 and latitudinal variability (Coustenis et al., 2013; 2016); future extended exploration of Titan
135 is necessary to get a full picture of the variations within this complex environment.

136 Titan is the only known planetary body, other than the Earth with long-standing liquid on
137 its surface, albeit hydrocarbons instead of water, likely fed by a combination of precipitation,
138 surface runoff and subsurface alkanofers (hydrocarbon equivalent of aquifers) in the icy crust
139 (Hayes et al., 2008). The presence of radiogenic noble gases in the atmosphere indicates some
140 communication between the surface and the subsurface and is suggestive of water-rock
141 interactions and methane outgassing processes (Tobie et al., 2012), possibly associated with
142 cryovolcanic activity or other exchange processes (Lopes et al., 2007, 2016; Solomonidou et
143 al., 2014, 2016). The detection of a salty ocean at an estimated 50-80 km depth (Iess et al.,
144 2012; Beghin et al., 2012; Mitri et al., 2014b) and the possible communication between this

145 ocean and the organic-rich surface hint at exciting astrobiological possibilities. While Cassini
146 has provided tantalizing views of the surface with its lakes and seas, dunes, equatorial
147 mountains, impact craters and possible cryovolcanos, its low resolutions make it difficult to
148 identify morphological features, to quantify geological processes and relationships between
149 different geological units and monitor changes due to geologic or atmospheric activity.
150 Constraining the level of geological activity on Titan is crucial to understanding its evolution
151 and determining if this ocean world could support abiotic/prebiotic activity.

152 Both Titan and Enceladus possess several, if not all, of the key ingredients necessary for
153 life: an energy source, liquid habitats, nutrients (organic compounds) and a liquid transport
154 cycle to move nutrients and waste (McKay et al., 2008, 2016). While sunlight is a minimal
155 source of energy for solid bodies in the outer Solar System, interior heat sources derived from
156 a rocky core or tidal forces produced by neighbouring satellites and planet can be quite
157 significant. Most recently, the Cassini INMS has identified molecular hydrogen (0.4-1.4%) in
158 Enceladus' plume (Waite et al., 2017) providing further evidence of water-rock interactions
159 which suggests that methane formation from CO₂ in Enceladus' subsurface ocean could occur
160 in a similar fashion as it occurs on Earth where extremophile microbes in hydrothermal sea
161 vents produce methane as a metabolic by-product (McKay et al., 2008). Another compelling
162 discovery is the complex large nitrogen-bearing organic molecules in Titan's upper
163 atmosphere by Cassini (Waite et al., 2007; Coates et al., 2007). The low resolution of the in-
164 situ mass spectrometers on Cassini, however, precludes the determination of the chemical
165 composition of this complex organic matter. In situ exploration with more advanced
166 instruments is required to investigate the prebiotic potential of Titan.

167 The discovery in 2005 of a plume emanating from multiple jets in Enceladus' south polar
168 terrain is one of the major highlights of the Cassini-Huygens mission (Figure 2) (Dougherty
169 et al., 2006; Porco et al., 2006; Spahn et al., 2006). Despite its small size (10 times smaller

170 than Titan), Enceladus is the most active moon of the Saturnian system. Although geyser-like
171 plumes have been observed on Triton (Soderblom et al., 1990) and more recently transient
172 water vapour activity around Europa has been reported (Roth et al., 2014; Sparks et al.,
173 2016,2017), Enceladus is the only satellite for which this activity is known to be endogenic in
174 nature. The jets, of which approximately one hundred have been identified (Porco et al.,
175 2014) form a huge plume of vapour and ice grains above Enceladus' south polar terrain and
176 are associated with elevated heat flow along tectonic ridges, called 'tiger stripes'. Enceladus'
177 endogenic activity and gravity measurements indicate that it is a differentiated body
178 providing clues to its formation and evolution (Iess et al., 2014). Sampling of the plume by
179 Cassini's instruments revealed the presence of water vapour, ice grains rich in sodium and
180 potassium salts (Postberg et al., 2011), organics, both in the gas (Waite et al., 2009) and in the
181 ice grains (Postberg et al., 2008, 2015), and molecular H (Waite et al., 2017). The jet sources
182 are connected to a subsurface salt-water reservoir that is likely alkaline in nature and
183 undergoing hydrothermal water-rock interactions (Porco et al., 2006, 2014; Waite et al., 2006,
184 2009, 2017; Postberg et al., 2009, 2011; Hsu et al., 2011, 2014; Glein et al., 2015). The
185 putative exothermic water-rock interactions on Enceladus could be further constrained by
186 quantifying He and constraining the amount of H₂ in the plume. Gravity, topography and
187 libration measurements demonstrate the presence of a global subsurface ocean (Iess et al.,
188 2014; McKinnon et al., 2015; Thomas et al., 2016). The co-existence of organic compounds,
189 salts, liquid water and energy sources on this small moon provides all necessary ingredients
190 for the emergence of life by chemoautotrophic pathways (McKay et al., 2008) – a generally
191 held model for the origin of life on Earth in deep sea vents.

192 Titan and Enceladus offer an opportunity to study analogous prebiotic processes that may
193 have led to the emergence of life on Earth. Retracing the processes that allowed the
194 emergence of life on Earth around 4 Ga is a difficult challenge since most traces of the

195 environmental conditions at that time have been erased. It is, therefore, crucial for
196 astrobiologists to find extraterrestrial planetary bodies with similarities to our planet,
197 providing a way to study some of the processes that occurred on the primitive Earth, when
198 prebiotic chemistry was active. The eruption activity of Enceladus offers a unique possibility
199 to sample fresh material emerging from subsurface liquid water and to understand how
200 exchange processes with the interior control surface activity. It provides us with an
201 opportunity to in-situ study phenomena that have been important in the past on Earth and
202 throughout the outer Solar System.

203 FIGURE 2

204

205 **3. Scientific Objectives and Investigations**

206 The scientific appeal of Titan and Enceladus have stimulated many previous mission studies
207 (e.g. see reviews by Lorenz, 2000; 2009) which have articulated detailed scientific objectives
208 for post-Cassini exploration (e.g. Tobie et al., 2014). At Titan, in particular, the diversity of
209 scientific disciplines (Dougherty et al., 2009) has prompted a variety of observing platforms
210 from orbiters (“Titan Explorer”, Leary et al., 2007; Mitri et al., 2014), landers for the seas
211 (“Titan-Saturn System Mission – TSSM”, Strange et al., 2009; “Titan Mare Explorer -
212 TiME”, Stofan et al., 2013; Mitri et al., 2014), landers for land (Titan Explorer), fixed-wing
213 aircraft (“AVIATR”, Barnes et al., 2012), balloons (Titan Explorer, TSSM and others).
214 Additionally, Enceladus’ plume has attracted designs of spacecraft to sample it: “Titan and
215 Enceladus Mission TANDEM” (Coustenis et al., 2009), “Journey to Enceladus and Titan –
216 JET” and “Enceladus Life Finder – ELF” (Reh et al., 2016). Similar to TANDEM, TSSM
217 and JET, E²T would address science goals at both targets.

218 The proposed E²T mission has two major goals and several science objectives (Table 1)
219 that would be pursued through Enceladus and Titan investigations. These investigations

220 would be conducted using the E²T mission model payload which consists of three
221 instruments: two time-of-flight mass spectrometers (TOF-MS), the Ion and Neutral Gas Mass
222 Spectrometer (INMS) and the Enceladus Icy Jet Analyzer (ENIJA) dust instrument; and a
223 high-resolution infrared (IR) camera, the Titan Imaging and Geology, Enceladus
224 Reconnaissance (TIGER). With considerable improvements in mass range, resolution and
225 sensitivity, as compared with Cassini, the INMS and the ENIJA time of flight mass
226 spectrometers would provide the data needed to decipher the subtle details of the aqueous
227 environment of Enceladus from plume sampling and of the varying complex pre-biotic
228 chemistry occurring in Titan's atmosphere. The Titan Imaging and Geology, Enceladus
229 Reconnaissance (TIGER) mid-wave infrared camera would map thermal emission from
230 Enceladus' tiger stripes at meter scales and investigate Titan's geology and compositional
231 variability at decameter scales, a resolution at least ten times better than Cassini. The
232 scientific payload will be described in Section 4.

233 While Cassini-Huygens and its extended missions have revealed much about Enceladus
234 and Titan, the spacecraft (S/C) was not equipped to search for life or constrain the evolution
235 of these ocean worlds. In-situ mass spectroscopic measurements by Cassini-Huygens at
236 Enceladus and Titan revealed a wealth of chemical complexity of neutral and positively
237 charged molecules. Those analyses, however, are limited by the low sensitivity, mass range,
238 and resolution of the Cassini-Huygens mass spectrometers limiting, for example, their ability
239 to resolve low-mass isobaric molecular species. For example, in Enceladus' vapour plume an
240 unidentified species with a mass-to-charge (m/z) ratio of 28, can be either CO, N₂, C₂H₄ or a
241 combination thereof. Determining the relative abundances of these different species is
242 essential to constraining the origin of volatiles on Enceladus and to assess whether they were
243 reprocessed internally. E²T mass spectrometers enable the separation of low-mass isobaric
244 interferences, for example ¹³C and ¹²CH and CO and N₂. Further, Cassini mass spectrometers

245 were limited to the study of only low-mass neutral and positive ions. The detection of heavy
246 complex negative ions in Titan's upper atmosphere by the Cassini Plasma Spectrometer
247 (CAPS), intended to detect electrons, was a surprising find that indicated complex coupling
248 processes between neutral and ionic molecules that lead to the formation of aerosols and
249 possibly to prebiotic activity. Negative water group ions were also detected in Enceladus'
250 plume (Coates et al., 2010). The high mass range/resolution and ability to detect anions of
251 E²T's mass spectrometers would constrain the nature and dynamics of these heavy
252 hydrocarbon and nitrile molecules.

253 The nature of the surfaces of Titan and Enceladus have been revealed by Cassini but only
254 at low to moderate resolutions with the exception of the Descent Imager /Spectral Radiometer
255 (DISR) onboard the Huygens probe that landed on Titan's surface on January 14, 2005,
256 which had a resolution ranging from 10 m at 10 km from the surface down to centimeters at
257 the surface giving an indication of the world waiting to be revealed by a new mission to the
258 Saturn system. Huygens' DISR was able to obtain images of a 25 m² area (Tomasko et al.,
259 2005). Data from Cassini Visual Infrared Mapping Spectrometer (VIMS) show that Titan is
260 visible at several near-infrared atmospheric windows. Scattering by aerosols in the
261 atmosphere, which limits the signal-to-noise ratio (SNR) and resolution of such data,
262 decreases at longer wavelengths. At 5 μm there is virtually no scattering from Titan's
263 atmospheric aerosols, allowing observations with spatial resolutions that are an order of
264 magnitude better than Cassini observations (Clark et al., 2010; Soderblom et al., 2012; Barnes
265 et al., 2014; Hayne et al., 2014; Sotin et al., 2016). Additionally, these data would be highly
266 sensitive to organic composition (Clark et al., 2010; Barnes et al., 2012). A high-resolution
267 map of Titan within the atmospheric windows at 1.3, 2 and 5 μm would enable E²T to
268 identify morphology not evident from Cassini data to quantify geological processes and
269 relationships between different geological units and monitor changes due to geologic or

270 atmospheric activity, such as erosion due to climatic changes or even transient features on the
271 lakes and seas of Titan. In addition, high-resolution IR imaging of Enceladus' south polar
272 terrain (both in reflected sunlight and in thermal emission) would provide new detail of the
273 tectonically active surface and constrain characteristics of the hydrothermal system by
274 determining the correlation between the spatial variations in plume composition (vapour and
275 icy grains) measured by the mass spectrometers and source activity.

276 **FIGURE 3**

277 The first scientific goal of E²T mission on Enceladus would focus on the origin and
278 evolution of volatile compounds in the plume vapour and icy grains. On Titan, the focus
279 would be on the origin and evolution of volatiles, the methane based cycle and evidence for
280 climate change. In addition, on Titan, there would be a focus on determining the major
281 processes controlling the distribution of atmospheric constituents, the impact the methane
282 cycle has on Titan's surface evolution and the morphological signatures of the internal
283 processes of Titan and surface-interior chemical communication. The second scientific goal
284 on Enceladus would examine the nature of hydrothermal activity and search for evidence of
285 abiotic/prebiotic processes. On Titan, the focus would be on discerning what level of
286 complexity abiotic/prebiotic chemistry has evolved.

287

288 **3.1 Origin and Evolution of Volatile-Rich Ocean Worlds in the Saturn System**

289 The formation of satellites around the gas giant planets Jupiter and Saturn is commonly
290 considered to be in many ways similar to the formation of a miniature version of the Solar
291 System. Satellites are created as by-products of planet formation within a circumplanetary
292 accretion disk of dust and gas (Estrada et al., 2009; Lunine et al., 2010). Their subsequent

293 evolution can be constrained by current chemical and isotopic abundances, satellite activity
294 whether it be endogenic or exogenic and present day internal structure and dynamics. The
295 Saturn system may have followed a more complex evolution than the Jupiter system, with the
296 disruption of lunar-size objects early during the system evolution and their re-accretion later
297 during the system evolution (Canup, 2010; Charnoz et al., 2011). A late accretion scenario
298 may explain the mass distribution and ice/rock ratio of the mid-sized moons and the existence
299 of the planet's ring. Such a scenario is supported by recent estimation of the dissipation factor
300 in Saturn, which is ten times smaller than initially anticipated (Lainey et al., 2012, 2016) and
301 which implies a rapid tidal evolution of the system. In this context, Enceladus may have
302 formed less than 1 billion years ago, while Titan may have accreted earlier. This may have
303 resulted in significant differences in their initial volatile inventory and their subsequent
304 evolution.

305 Whether the volatiles currently present on Titan and Enceladus are primordial, originating
306 in the solar nebula or Saturnian subnebula possibly altered during the accretion process or
307 else were produced in some secondary manner is still being debated (e.g., Atreya et al.,
308 2006). Photochemical processes on Titan and aqueous alteration on Enceladus have affected
309 the initial volatile inventory to an extent unknown. By combining in-situ chemical analysis of
310 Titan's atmosphere and Enceladus' plume with observations of Enceladus' plume dynamics
311 and Titan's surface geology, E²T would provide clues on how the ocean worlds acquired their
312 initial volatile inventory and how it was subsequently modified during their evolution, which
313 would provide clues to an understanding of the nature of Saturn subnebula formation
314 conditions and its subsequent evolution, the conditions of the early solar nebula, the nature of
315 cometary and giant impacts, all of which might also help to predict the physical and chemical
316 properties of terrestrial planets and exoplanets beyond the Solar System.

317

318 *3.1.1 Chemical Constraints on the Origin and Evolution of Titan and Enceladus*

319 The origin and evolution of Titan's methane still needs to be constrained. Whether Titan's
320 methane is primordial likely through water-rock interactions in Titan's interior during its
321 accretionary phase (Atreya et al., 2006) or else delivered to Titan during its formation
322 processes (Mousis et al., 2009) or by cometary impacts (Zahnle et al., 1992; Griffith and
323 Zahnle, 1995) is a key open question. On Titan, the Huygens probe detected small argon
324 abundance (^{36}Ar) and a tentative amount of neon (^{22}Ne) in its atmosphere (Niemann et al.,
325 2005, 2010), but was unable to detect the corresponding abundance of xenon and krypton.
326 The presence of ^{22}Ne ($^{36}\text{Ar} / ^{22}\text{Ne} \sim 1$) was unexpected as neon is not expected to be present in
327 any significant amounts in protosolar ices (Niemann et al., 2005, 2010) and may indicate
328 water-rock interactions and outgassing processes (Tobie et al., 2012). The non-detection of
329 xenon and krypton supports the idea that Titan's methane was generated by serpentinization
330 of primordial carbon monoxide and carbon dioxide delivered by volatile depleted
331 planetesimals originating from within Saturn's subnebula (e.g., Atreya et al., 2006). To
332 support a primordial methane source, xenon and krypton both would have to be sequestered
333 from the atmosphere. While xenon is soluble in liquid hydrocarbon (solubility of 10^{-3} at 95 K)
334 and could potentially be sequestered into liquid reservoirs, argon and krypton cannot (Cordier
335 et al., 2010). Therefore, the absence of measureable atmospheric krypton requires either
336 sequestration into non-liquid surface deposits, such as clathrates (Mousis et al., 2011), or
337 depletion in the noble gas concentration of the planetesimals (Owen and Niemann, 2009).
338 Unlike Cassini INMS, the E²T INMS has the mass range and the sensitivity to accurately
339 measure xenon. E²T would measure the abundance of noble gases in the upper atmosphere of
340 Titan to discriminate between crustal carbon sequestration and carbon delivery via depleted
341 planetesimals.

342 The longevity of methane in Titan's atmosphere is still a mystery. The value of $^{12}\text{C}/^{13}\text{C}$ in
343 Titan's atmosphere has been used to conclude that methane outgassed $\sim 10^7$ years ago (Yung
344 et al., 1984), and is being lost via photolysis and atmospheric escape (Yelle et al., 2008). It is
345 an open question whether the current methane rich atmosphere is a unique event, in a steady
346 state where methane destruction and replenishment are in balance (Jennings et al., 2009), or is
347 a unique transient event and is in a non-steady state where methane is being actively depleted
348 or replenished. Indeed, the possibility that Titan did not always possess a methane rich
349 atmosphere seems to be supported by the fact that the amount of ethane on Titan's surface
350 should be larger than the present inventory; though Wilson and Atreya (2009) contend that
351 missing surface deposits may simply be reburied into Titan's crust and Mousis and Schmitt
352 (2008) have shown that it is possible for liquid ethane to react with a water-ice and methane-
353 clathrate crust to create ethane clathrates and release methane. Nixon et al. (2012), however,
354 favours a model in which methane is not being replenished and suggest atmospheric methane
355 duration is likely between 300 and 600 Ma given that Hörst et al. (2008) demonstrated that
356 300 Ma is necessary to create Titan's current CO inventory and recent surface age estimates
357 based on cratering (Neish and Lorenz, 2012). Mandt et al. (2012) suggests that methane's
358 presence in the atmosphere, assumed here to be due to outgassing, has an upper limit of 470
359 Ma or else up to 940 Ma if the presumed methane outgassing rate was large enough to
360 overcome $^{12}\text{C}/^{13}\text{C}$ isotope fractionation resulting from photochemistry and escape. Both the
361 results of Mandt et al. (2012) and Nixon et al. (2012) fall into the timeline suggested by
362 interior models (Tobie et al., 2006) which suggests that the methane atmosphere is the result
363 of an outgassing episode that occurred between 350 and 1350 Ma. On Titan, both simple
364 (methane, ethane and propane) and complex hydrocarbons precipitate out of the atmosphere
365 onto the surface. Measuring the isotopic ratios ($^{14}\text{N}/^{15}\text{N}$; $^{12}\text{C}/^{13}\text{C}$; D/H; $^{16}\text{O}/^{18}\text{O}$; $^{17}\text{O}/^{16}\text{O}$) and
366 abundances of the simple alkanes (e.g., methane, ethane and propane) would constrain the

367 formation and evolution of the methane cycle on Titan. Further measurements of radiogenic
368 noble gases such as ^{40}Ar and ^{22}Ne , which are typically markers of volatile elements from
369 Titan's interior can constrain outgassing episodes. Detection of ^{40}Ar and tentatively ^{22}Ne in
370 the atmosphere has provided circumstantial evidence of water-rock interactions and methane
371 outgassing from the interior (Niemann et al., 2010; Tobie et al., 2012). Recent measurements
372 by ground-based observatories including measurements of CO and its carbon and oxygen
373 isotopologues accompanied by the first detection ^{17}O in Titan and indeed in the outer Solar
374 System by Atacama Large Millimeter/submillimeter Array (ALMA) can be followed up on in
375 more detail by in-situ spectroscopic measurements (Serigano et al., 2016). E²T would
376 measure the composition and isotopic ratios of Titan's upper atmosphere to determine the age
377 of methane in the atmosphere and characterize outgassing history.

378 On Enceladus, Cassini measurements by INMS (Waite et al., 2006, 2009, 2017) and UVIS
379 (Hansen et al., 2006, 2008) showed that plume gas consists primarily of water vapour with a
380 few percent other volatiles. In addition to H_2O , as the dominant species, INMS was able to
381 identify CO_2 (0.3-0.8%), CH_4 (0.1-0.3%), NH_3 (0.4-1.3%) and H_2 (0.4-1.4%), in the vapour
382 plume as well as an unidentified species with a mass-to-charge (m/z) ratio of 28, which is
383 thought to be either N_2 or C_2H_4 or a combination of these compounds or CO. The low mass
384 resolution of Cassini INMS is insufficient to separate these species, and the UVIS
385 measurements can only provide upper limits on N_2 and CO abundance. Determining the
386 abundance ratio between these different species is, however, essential to constrain the origin
387 of volatiles on Enceladus and to assess if they were internally reprocessed. A high CO/N_2
388 ratio, for instance, would suggest a cometary-like source with only a moderate modification
389 of the volatile inventory, whereas a low CO/N_2 ratio would indicate a significant internal
390 reprocessing.

391 In addition to these main volatile species, the possible presence of trace quantities of C_2H_2 ,

392 C₃H₈, methanol, formaldehyde and hydrogen sulphide has been detected within the INMS
393 data recorded during some Cassini flybys (Waite et al., 2009). Organic species above the
394 INMS mass range of 99 u are also present but could not be further constrained (Waite et al.,
395 2009). The identification and the quantification of the abundances of these trace species
396 remains very uncertain due to the limitations of the mass spectrometer onboard Cassini.

397 Except for the measurement of D/H in H₂O on Enceladus (which has large uncertainty,
398 Waite et al., 2009), no information is yet available for the isotopic ratio in Enceladus' plume
399 gas. The E²T mission would determine the isotopic ratios (D/H, ¹²C/¹³C, ¹⁶O/¹⁸O, ¹⁴N/¹⁵N) in
400 major gas compounds of Enceladus' plume as well as ¹²C/¹³C in organics contained in icy
401 grains. Comparison of gas isotopic ratios (e.g., D/H in H₂O and CH₄, ¹²C/¹³C in CH₄, CO₂, and
402 CO; ¹⁶O/¹⁸O in H₂O, CO₂, CO; ¹⁴N/¹⁵N in NH₃ and N₂) and with Solar System standards would
403 provide essential constraints on the origin of volatiles and how they may have been internally
404 reprocessed. Simultaneous precise determination of isotopic ratios in N, H, C and O- bearing
405 species in Enceladus' plume and Titan's atmosphere would permit a better determination of
406 the initial reference values and a quantification of the fractionation due to internal and
407 atmospheric processes on both moons.

408 Noble gases also provide essential information on how volatiles were delivered to
409 Enceladus and if significant exchanges between the rock phase and water-ice phase occurred
410 during Enceladus' evolution. The E²T mission would be able to determine the abundance of
411 ⁴⁰Ar, expected to be the most abundant isotope, as well as the primordial (non-radiogenic)
412 argon isotopes, ³⁶Ar and ³⁸Ar. The detection and quantification of ³⁶Ar and ³⁸Ar would place
413 fundamental constraints on the volatile delivery in the Saturn system. A low ³⁶Ar/N₂ ratio, for
414 instance, would indicate that N₂ on Enceladus is not primordial, like on Titan (Niemann et al.,
415 2010), and that the fraction of argon brought by cometary materials on Enceladus is rather

416 low. In addition to argon, if Ne, Kr, and Xe are present in detectable amounts, E²T would be
417 able to test whether primordial noble gases on Enceladus were primarily brought by a
418 chondritic phase or cometary ice phase, which has implications for all the other primordial
419 volatiles. The ⁴⁰Ar/³⁸Ar/³⁶Ar as well as ²⁰N/²¹Ne/²²Ne ratios would also allow for testing of
420 how noble gases were extracted from the rocky core. Abundance ratios between Ar/Kr and
421 Ar/Xe, if Kr and Xe are above detection limit, would offer an opportunity to test the influence
422 of clathration storage and decomposition in volatile exchanges through Enceladus's ice shell.

423 The origin of methane detected in Enceladus' plume is still uncertain. Methane, ubiquitous
424 in the interstellar medium was most likely embedded in the protosolar nebula gas. The inflow
425 of protosolar nebular gas into the Saturn subnebula may have trapped methane in clathrates
426 that were embedded in the planetesimals of Enceladus during their formation. Alternatively,
427 methane may have been produced via hydrothermal reactions in Enceladus' interior; a
428 possibility made more evident by the recent discovery of molecular hydrogen in Enceladus'
429 plume (Waite et al., 2017). Mousis et al. (2009) suggests that if the methane of Enceladus
430 originates from the solar nebula, then Xe/H₂O and Kr/H₂O ratios are predicted to be equal to
431 $\sim 7 \times 10^{-7}$ and 7×10^{-6} in the satellite's interior, respectively. On the other hand, if the methane
432 of Enceladus results from hydrothermal reactions, then Kr/H₂O should not exceed $\sim 10^{-10}$ and
433 Xe/H₂O should range between $\sim 1 \times 10^{-7}$ and 7×10^{-7} in the satellite's interior. The E²T mission
434 by performing in situ analysis with high-resolution mass spectrometry of both the vapour and
435 solid phases would quantify the abundance ratios between the different volatile species
436 present in the plume of Enceladus, the isotopic ratios in major species, and the noble gas
437 abundance.

438

439 *3.1.2 Sources and Compositional Variability of Enceladus' Plume*

440 The detection of salty ice grains (Postberg et al., 2009, 2011), the high solid/vapour ratio
441 (Porco et al., 2006; Ingersoll and Ewald, 2011), and the observations of large particles in the
442 lower part of the plume (Hedman et al., 2009) all indicate that the plume of Enceladus
443 originates from a liquid source likely from the subsurface ocean rather than from active
444 melting within the outer ice shell (Figure 3). However, the abundance of the major gas
445 species observed by Cassini suggests some contribution from the surrounding cold icy crust
446 should also be considered. If plume gases exclusively originate from a liquid water reservoir,
447 low-solubility species would be more abundant than high-solubility compounds, which is not
448 apparent in the INMS data. Cassini observations show that the plume is made up of ~100
449 discrete collimated jets as well as a broad, diffuse component (Hansen et al., 2008, 2011;
450 Postberg et al., 2011; Porco et al., 2014). The majority of plume material is found in the
451 distributed diffuse portion of the plume while only a small portion of gas and grains are
452 emitted from the jets (Hansen et al., 2011; Postberg et al., 2011). The saltiness of the ice
453 grains and the recent detections of nanometer sized silica dust in E-ring particles, which are
454 believed to come from Enceladus (Hsu et al., 2011, 2015), and molecular hydrogen in
455 Enceladus' plume (Waite et al., 2017) all indicate their origin is a location where alkaline
456 high temperature hydrothermal reactions and likely water-rock interactions are occurring.

457 **FIGURE 3**

458 Although the Cassini (Cosmic Dust Analyzer) CDA has constrained knowledge of plume
459 compositional stratigraphy, measurements of the absolute abundance and composition of
460 organics, silicates and salts are poorly constrained given the low spatial resolution (10 km),
461 low mass resolution and limited mass range of the CDA. The E²T ENIJA is capable of
462 providing a spatial accuracy of less than 100 m, allowing for a precise determination of
463 compositional profiles along the spacecraft trajectory (Srama et al., 2015). The Cassini INMS

464 provided only plume integrated spectra and is not able to separate gas species with the same
465 nominal mass. E²T INMS' high mass resolution, which is 50 times larger than that of Cassini
466 INMS, would allow for separation of isobaric interferences, for example separating ¹³C and
467 ¹²CH and CO and N₂. Determining high-resolution spatial variations in composition is crucial
468 to establish whether the jets are fed by a common liquid reservoir or if jet sources are
469 disconnected, and if the local liquid sources interact with a heterogeneous in the icy crust.
470 Variations in composition between the solid and gas phases as a function of distance from jet
471 sources can also provide information about how the less volatile species condense on the
472 grains, thus constraining the eruption mechanisms. The E²T mission would allow for the
473 determination of the compositional distribution between both solid and vapour phases of
474 Enceladus' plume, thus providing crucial constraints on the nature and composition of the jet
475 sources, and on the relative contributions of subsurface liquid reservoirs and the surrounding
476 cold icy crust. Spatial variations in composition within the plume and possible correlations
477 with the jet sources would permit for testing if the volatile compounds originate from a
478 common reservoir and how the less volatile compounds are integrated in the solid particles
479 during the eruption processes.

480

481 *3.1.3 Geological Constraints on Titan's Methane Cycle and Surface Evolution*

482 As discussed above, there is an open question whether Titan's methane-rich atmosphere is
483 being actively replenished, or if methane is being lost and Titan's methane may eventually be
484 depleted (Yung et al., 1984). Cryovolcanism has been suggested as a mechanism by which
485 methane and argon can be transported from Titan's interior to its surface (e.g., Lopes et al.,
486 2013). Cryovolcanic activity may also promote methane outgassing (Tobie et al., 2006);
487 while methane clathrates are stable in Titan's ice shell in the absence of destabilizing thermal

488 perturbations and/or pressure variation, variations in the thermal structure of Titan's outer ice
489 shell during its evolution could have produced thermal destabilization of methane clathrates
490 generating outgassing events from the interior to the atmosphere (Tobie et al., 2006; see also
491 Davies et al., 2016). A number of candidate cryovolcanic features have been identified in
492 Cassini observations (Lopes et al., 2013). E²T TIGER high-resolution colour images would
493 provide the data needed to determine the genesis of these features. Stratigraphic relationships
494 and crater counting would provide a means by which the relative ages of these features may
495 be constrained.

496 A related question to the age of Titan's atmosphere is if Titan's climate is changing. At
497 present, most of the observed liquid methane is located in the north polar region (Aharonson
498 et al., 2009). There have been suggestions, however, that organic seas may have existed in
499 Titan's tropics (Moore and Howard, 2010; MacKenzie et al., 2014), and/or in broad
500 depressions in the south (Aharonson et al., 2009; Hayes et al., 2011). Observations and
501 models suggest Titan's methane distribution varies on seasonal timescales (e.g., Waite et al.,
502 2007; Hayes et al., 2010; Turtle et al., 2011; Coustenis et al., 2013, 2016) or Milankovitch
503 timescales (Aharonson et al., 2009). Alternative models suggest that methane is being
504 depleted and Titan's atmosphere is drying out (Moore and Howard, 2010). High-resolution
505 images of the margins and interiors of these basins would allow us to determine if they once
506 held seas. Identification of impact features or aeolian processes within these basins would
507 help to constrain the timing of their desiccation.

508 In addition to their inherent scientific interest, Titan's dunes also serve as a witness plate to
509 climatic evolution. Larger duneforms take longer to form than smaller duneforms. In Earth's
510 Namib desert, these differing timescales result in large, longitudinal dunes that adhere to the
511 overall wind conditions from the Pleistocene 20,000 years ago, while smaller superposing

512 dunes (sometimes called rake dunes, or flanking dunes) have responded to the winds during
513 our current interglacial and orient ages accordingly. On Titan, E²T TIGER's superior spatial
514 resolution would resolve these potential smaller dunes on top of the known longitudinal
515 dunes, and would therefore reveal if Titan's recent climate has been stable or if it has changed
516 over the past few Ma. The E²T mission would provide high-resolution colour imaging of
517 Titan that can be used to characterize candidate cryovolcanic features that could be
518 replenishing Titan's atmosphere and paleo-seas or dune patterns that evidence changes in
519 Titan's climate.

520 Understanding climate change on Titan would provide insight that may be relevant to the
521 future of our own planet, when surface conditions with warm tropospheric temperatures will
522 preclude stable equatorial/mid-latitude oceans and the liquid water will be limited to the
523 poles, while at the equator, occasional intense rainstorms might scour out fluvial features, but
524 the principle sedimentary deposits will be sand dunes. The closest analogous in our solar
525 system to such a future Earth is Titan (Coustenis et al., 2009). Indeed, the evolution of the solar
526 luminosity makes it almost unavoidable that, in ~ 0.5 -1 Ga from now, the tropopause temperature of
527 the Earth will be elevated to the point that loss of the Earth's oceans by evaporation and then
528 stratospheric photolysis of the water vapour will occur over a timescale of the order a hundred million
529 years. From that point on, surface liquid water will be limited to the poles, will have a short
530 photochemical lifetime, and if persistent would be resupplied by mantle/deep crustal water. At the
531 equator, occasional intense rainstorms might scour out fluvial features, but the principle sedimentary
532 deposits will be sand dunes.

533 Titan's geology is unique in that liquid and solid organics likely play key roles in many of
534 the observed processes. These processes, in turn, play an important role in modifying these
535 organics, both physically and chemically. Understanding these modification processes is
536 crucial to investigating the complex chemistry occurring on this moon. Furthermore, study of

537 Titan's geology allows us to investigate processes that are common on Earth, but in
538 drastically different environmental conditions, providing a unique way to gain insight into the
539 processes that shaped the Earth and pre-Noachian Mars.

540 Observations of Titan suggest the landscape is significantly modified by liquid organics
541 (e.g., Tomasko et al., 2005; Soderblom et al., 2007; Burr et al., 2013). Fluvial erosion is
542 observed at all latitudes, with a variety of morphologies suggesting a range of controls and
543 fluvial processes (Burr et al., 2013). High-resolution color imaging would provide insight into
544 the nature of this erosion: whether it is predominantly pluvial or sapping in nature and
545 whether it is dominated by mechanical erosion or dissolution. Dissolution processes are also
546 suspected to control the landscape of Titan's labyrinth terrains (Cornet et al., 2015) and may
547 be responsible for the formation of the polar sharp edged depressions (Hayes et al., 2008):
548 E²T imaging would allow direct testing of these hypotheses.

549 Both fluvial and aeolian processes likely produce and transport sediments on Titan. Dunes
550 are observed across Titan's equator (e.g., Radebaugh et al., 2008; Malaska et al., 2016) while
551 a variety of fluvial sediment deposits have been identified across Titan (e.g., Burr et al., 2013;
552 Birch et al., 2016). Detailed images of the margins of the dune fields would allow us to
553 determine the source and fate of sands on Titan. E²T images would also help determine
554 whether the observed fluvial features are river valleys or channels (cf. Burr et al., 2013)
555 providing key information in obtaining accurate discharge estimates needed to model
556 sediment transport (Burr et al., 2006). E²T observation would provide insight into the primary
557 erosion processes acting on crater rims, which likely comprise a mixture of organics and
558 water ice (cf. Neish et al., 2015, 2016). Finally, E²T imagining may provide insight into the
559 nature of erosion that exists in Titan's mid-latitudes, a region that shows little variability in
560 Cassini observations.

561 Of great interest in understanding the evolution of Titan's surface is determining the nature
562 of the observed geologic units, including their mechanical and chemical properties. Fluvial
563 processes, the degree to which mechanical versus dissolution dominates and the existence of
564 sapping, reflect the material properties of the surface and therefore can be used as a powerful
565 tool to investigate the properties of the surface. E²T imaging would also allow us to
566 investigate the strength of the surface materials by constraining the maximum slopes
567 supported by different geologic units. Detailed color and stereo imaging of the boundaries of
568 units would also allow investigation of the morphology, topography, and spectral relationship
569 across unit boundaries. E²T would take high-resolution color images of Titan that would
570 elucidate the nature of the geological evolution of Titan's organic-rich surface.

571

572 **3.2 Habitability and Potential for Life in Ocean Worlds, Enceladus and Titan**

573 Ocean worlds, such as Titan and Enceladus, are the subjects of great astrobiological interest
574 as water is one of the key requirements for life as we know it (Lammer et al., 2009).
575 Additionally, the organic surface environment of Titan provides an ideal, and in many ways
576 unique setting to investigate the prebiotic chemistry that may have led to the emergence of
577 life on the Earth. Water in ocean worlds in the outer Solar System is found beneath the
578 surface of an insulating ice shell, that regulates heat and chemical transport.

579 The dissipation of energy from tidal flexing, combined with radiogenic energy from these
580 moons' interiors provide the energy to sustain an ocean. The presence of antifreeze elements,
581 such as salts or ammonia, suggested by mass spectrometric measurements on Titan and
582 Enceladus (Niemann et al., 2005; Waite et al., 2009) and accretion models (Lunine and
583 Steveson, 1987; Mousis et al., 2002) may also play an important role in sustaining these
584 subsurface oceans. Subsurface oceans are known to exist on both Titan and Enceladus based

585 on Cassini's mission gravity, shape and libration data (Iess et al, 2010, 2012, 2014; Mitri et
586 al, 2014b; McKinnon et al, 2015; Thomas et al, 2016), compositional in-situ measurements
587 and thermal evolution models (Tobie et al., 2005, 2006; Mitri and Showman, 2008; Mitri et
588 al., 2010). Enceladus is unique since water exchange is known to exist between the surface
589 and subsurface and, quite conveniently, this water is ejected into space for easy in situ
590 sampling. Titan provides its own unique environment in which a rich array of complex
591 organics exist on the surface and may interact with the subsurface ocean via cryovolcanic
592 activity or, alternatively, with transient liquid water at the surface following impact events.

593 Because the presence of a subsurface ocean decouples the interior from the outer ice shell,
594 there is a much larger deflection of the ice shell and thus enhanced tidal heating and stresses
595 in the shell; therefore tectonic features are much more likely present on ocean worlds (Mitri
596 et al., 2010; Nimmo and Pappalardo, 2016) than on icy satellites without subsurface oceans.
597 Surface geological activity may also lead to transport of surface organic material emplaced
598 via precipitation from the atmosphere on Titan or lodged in the surface as a result of cometary
599 impacts into subsurface oceans. Titan's hydrocarbon cycle and the associated meteorology
600 creates a global distribution of trace species, evident in the formation and dynamics of clouds
601 and an extensive photochemical haze in Titan's atmosphere, which affects the dynamics of
602 how, when and where organic material settles on the surface and possibly interacts with the
603 subsurface. In addition, cometary impacts could deliver key organics such as glycine, the
604 simplest amino acid which has been detected on both comet 67P/Churyumov-Gerasimenko
605 from in-situ sampling by ESA's Rosetta mission (Altwegg et al. 2016) and comet 81P/Wild-2
606 from samples returned by NASA's Stardust mission (Elsila et al. 2009). Transient liquid
607 water environments, created by impact melts could be an incubator for the deposited aerosols
608 to create prebiotic chemistry (Neish et al., 2010). Further it is likely that such impact melt
609 pools could be stable for 10^2 - 10^4 years (O'Brien et al., 2005). This process could be circular;

610 Tobie et al. (2012) suggests that some of the species now present in Titan's atmosphere may
611 have originally been dissolved in the subsurface. On smaller ocean worlds such as Europa
612 and Enceladus, the ocean may be in direct contact with the silicate core providing a means of
613 water-rock interactions (Mitri and Showman, 2005; Iess et al., 2014). As discussed above,
614 detection of nanometer silica dust particles in Saturn's E-ring (Hsu et al., 2015) and
615 molecular hydrogen in Enceladus' plume (Waite et al., 2017) strongly suggest water-rock
616 interactions within Enceladus. The enormous heat output in the south polar terrain, associated
617 with liquid water in contact with rocks, favours prebiotic processes, providing both an energy
618 source and mineral surfaces for catalyzing chemical reactions.

619 Titan and Enceladus, have already demonstrated remarkable astrobiological potential as
620 evidenced by Titan's complex atmosphere and methane cycle, analogous to Earth's water
621 cycle, and Enceladus' cryovolcanic plume spewing rich organics from the subsurface out into
622 space. Studies of the nature of these organics could tell us whether or not they are biogenic.
623 For instance, part of the CH₄ detected in the plume of Enceladus may result from
624 methanogens analogous to those occurring in anaerobic chemosynthetic ecosystems on Earth
625 (Stevens and McKinley, 1995; McKay et al., 2008); molecular hydrogen in Enceladus' plume
626 makes the occurrence of methanogenesis more likely (Waite et al., 2017). A powerful method
627 to distinguish between biogenic and abiogenic CH₄ is to analyze the difference in carbon
628 isotope, ¹²C/¹³C, between CH₄ and a potential source of C, most likely CO₂ on Enceladus and
629 Titan, and to analyze the pattern of carbon isotopes in other hydrocarbons, such as C₂H₆,
630 C₂H₄, C₂H₂, C₃H₈ etc. (Sherwood et al., 2002; McKay et al., 2008). The abundances of other
631 non-methane hydrocarbons relative to methane could also be used to distinguish between
632 biological and other sources (McKay et al., 2008; McKay, 2016). The detection of amino
633 acids could provide additional evidence for active biogenic processes; although they can be
634 produced, both biologically and via aqueous alteration of refractory organics, their

635 distribution pattern can confirm if they are of biological origin (Dorn et al., 2011). Indeed,
636 low molecular weight amino acids, such as glycine and alanine, are kinetically favorable and
637 therefore dominate mixture of amino acids synthesized by abiotic process, whereas amino
638 acids resulting from biotic process show a more varied distribution dominated by the protein
639 amino acids in roughly equal proportions (Dorn et al., 2011).

640 By searching for abnormal isotopic ratios and mass distribution of organic molecules,
641 including amino acids, E²T would determine what chemical processes control the formation
642 and evolution of complex organics on Titan and would test if biotic processes are currently
643 occurring inside Enceladus. The analysis of salts and minerals embedded in icy grains and
644 their possible distribution throughout the plume would constrain the nature of hydrothermal
645 activity occurring in Enceladus' deep interior and on how it connects with the plume activity.
646 The observations of Titan's surface would determine if complex organics have been in
647 contact with fresh water, either at the surface via cryovolcanism or impact melt, and/or if
648 material is actively being exchanged between the surface and interior.

649 .

650

651 **3.2.1 Evidence for Prebiotic and Biotic Chemical Processes on Titan and Enceladus**

652 Unlike the other ocean worlds in the Solar System, Titan has a substantial atmosphere,
653 consisting of approximately 95% nitrogen and 5% methane with trace quantities of
654 hydrocarbons such as ethane, acetylene, and diacetylene, and nitriles, including hydrogen
655 cyanide (HCN) and cyanogen (C₂N₂). Somewhat more complex molecules such as
656 cyanoacetylene, vinyl and ethylecyanide follow from these simpler units. In Titan's upper
657 atmosphere, Cassini has detected large organic molecules with high molecular masses over
658 100 u. In-situ measurements by the Cassini Plasma Spectrometer (CAPS) detected heavy

659 positive ions (cations) up to 400 u (Crary et al., 2009) and heavy negative ions (anions) with
660 masses up to 10,000 u (Coates et al., 2007) in Titan's ionosphere. Whereas Cassini INMS
661 only had the ability to detect cations, E²T INMS can detect both cations and anions and can
662 do so with much better mass resolution than Cassini-INMS (and a fortiori than Cassini-
663 CAPS). It is thought that these heavy negative ions, along with other heavy molecules found
664 in the upper atmosphere, are likely the precursors of aerosols that make up Titan's signature
665 orange haze, possibly even precipitating to the surface. While the compositions of these
666 molecules are still unknown, their presence suggest a complex atmosphere that could hold the
667 precursors for biological molecules such as those found on Earth. The ability to detect
668 prebiotic molecules in Titan's atmosphere is currently limited by the mass range of the
669 Cassini INMS to the two smallest biological amino acids, glycine (75 u) and alanine (89 u),
670 and the limited mass resolution precludes any firm identification. While Cassini INMS has
671 not detected 75 or 89 u molecules, it has detected positive ions at masses of 76 u and 90 u,
672 which are consistent with protonated glycine and alanine, respectively (Vuitton et al., 2007;
673 Hörst et al., 2012). Experimental results from a Titan atmosphere simulation experiment
674 found 18 molecules that could correspond to amino acids and nucleotide bases (Hörst et al.,
675 2012). The E²T mission would use high-resolution mass spectrometry to measure heavy
676 neutral and ionic constituents up to 1000 u, and the elemental chemistry of low-mass organic
677 macromolecules and aerosols in Titan's upper atmosphere as well as monitor neutral-ionic
678 chemical coupling processes.

679 The plume emanating from Enceladus' south pole probably contains the most accessible
680 samples from an extra-terrestrial liquid water environment in the Solar System. The plume is
681 mainly composed of water vapour and trace amounts of other gases: 0.3-0.8% CO₂, 0.1-0.3%
682 CH₄, 0.4-1.3% NH₃ and 0.4-1.4% H₂ (Waite et al., 2017). In addition, higher molecular
683 weight compounds with masses exceeding 100 u, were detected in the plume emissions

684 (Waite et al., 2009; Postberg et al., 2015). The presence of CO₂, CH₄ and H₂ can constrain the
685 oxidation state of Enceladus' hydrothermal system during its evolution. The minor gas
686 constituents in the plume are indicative of high-temperature oxidation-reduction (redox)
687 reactions in Enceladus' interior possibly a result of decay of short-lived radionuclides
688 (Schubert et al., 2007). In addition, H₂ production and escape may be a result of redox
689 reactions indicative of possible methanogenesis similar to the process occurring in terrestrial
690 submarine hydrothermal vents (McKay et al., 2008; Waite et al., 2017). Further, the high
691 temperatures and H₂ escape may have led to the oxidation of NH₃ to N₂ (Glein et al., 2008).
692 Detection and inventory of reduced and oxidized species in the plume material (e.g., NH₃/N₂
693 ratio, H₂ abundance, reduced versus oxidized organic species) can constrain the redox state
694 and evolution of Enceladus' hydrothermal system.

695 Cassini CDA measurements identified three types of grains in the plume and Saturn's E-
696 ring. Type I and Type II grains are both salt-poor (Figure 4). Type I ice grains are nearly
697 pure-water ice while Type II grains also possess silicates and organic compounds and Type
698 III grains are salt-rich (0.5–2.0% by mass) (Postberg et al., 2009, 2011). The salinity of these
699 particles suggests they originate in a place where likely water-rock interactions are taking
700 place.

701 **FIGURE 4**

702 Hsu et al. (2015) suggest that the ocean should be convective in order to have silica
703 nanoparticles transported from hydrothermal sites at the rocky core up to the surface of the
704 ocean where they can be incorporated into icy plume grains (Hsu et al. (2015)). To confirm
705 this hypothesis of current hydrothermal activity on Enceladus, a direct detection of silica and
706 other minerals within ejected ice grains is required. SiO₂ nano-particles detected in Saturn's
707 E-ring could be much better investigated and quantified by E²T ENIJA given its high

708 dynamic range (10^6 - 10^8). By performing high-resolution mass spectrometry of ice grains in
709 Enceladus' plume, the E²T mission would characterize the composition and abundance of
710 organics, salts and other minerals embedded in ice grains, as messengers of rock/water
711 interactions. It would also search for signatures of on-going hydrothermal activities from
712 possible detection of native He and further constrain recent measurements of native H₂ found
713 in Enceladus' plume (Waite et al., 2017).

714

715 **3.2.2 Physical Dynamics in Enceladus' Plume and Links to Subsurface Reservoirs**

716 The total heat emission at Enceladus' tiger stripes is at least 5 GW -possibly up to 15 GW,
717 (Howett et al., 2011), and in some of the hot spots where jets emanate, the surface
718 temperatures are as high as 200 K (Goguen et al., 2013). Cassini observations show that the
719 plume is made up of approximately 100 discrete collimated jets as well as a diffuse
720 distributed component (Hansen et al., 2008, 2011; Postberg et al., 2011; Porco et al., 2014).
721 The majority of plume material can be found in the distributed diffuse portion of the plume,
722 which likely originates from elongated fissures along Enceladus' tiger stripes while only a
723 small portion of gas and grains are emitted from the jets (Hansen et al., 2011; Postberg et al.,
724 2011). CDA measurements demonstrate that the majority of salt-poor grains tend to be
725 ejected through the jets and at faster speeds while larger salt-rich grains tend to be ejected
726 more slowly through the distributed portion of the plume (Postberg et al., 2011). The ice to
727 vapour ratio can constrain how Enceladus' plume material is formed and transported to the
728 surface. For example, ice/vapour ratios > 0.1–0.2 would exclude plume generation
729 mechanisms that require a large amount of ice grains to be condensed from vapour (Porco et
730 al., 2006; Ingersoll and Pankine, 2011). However, this ratio is poorly constrained with
731 estimates ranging from 0.05 (Schmidt et al., 2008) to 0.4 (Porco et al., 2006) to 0.35–0.7

732 (Ingersoll and Ewald, 2011). E²T high-resolution IR images and ENIJA can help constrain
733 this important ratio. Cassini ISS images used to track plume brightness variation, which is
734 proportional to the amount of grains in the plume, with the orbital position of Enceladus
735 found more ice grains are emitted when Enceladus is near its farthest point from Saturn
736 (apocenter). It is not understood if the plume vapour has such a variation. This temporal
737 variation of the plume indicates that it is tidally driven but could also be due to possible
738 physical libration (Hurford et al., 2009; Kite et al., 2016). Most recently, Kite et al. (2016)
739 has suggested that the tiger stripe fissures are interspersed with vertical pipelike tubes with
740 wide spacing that extend from the surface to the subsurface water. This mechanism allows
741 tidal forces to turn water motion into heat, generating enough power to produce eruptions in a
742 sustained manner. TIGER can provide high spatial resolution thermal emissions maps to
743 constrain the amount of energy dissipated between the tiger stripes. The E²T mission would
744 use high resolution IR imaging of the south polar terrain and mass spectra of the grains to
745 provide new details of its surface and constrain the links between plume activity, subsurface
746 reservoirs and deep hydrothermal processes.

747

748 **3.2.3 Geological Evidence for Interior-Surface Communication on Titan**

749 Geological processes such as tectonism and cryovolcanism indicate communication between
750 the surface and subsurface. While Titan's surface offers a wealth of geological processes, the
751 Cassini data lack the resolution needed in which to constrain the detailed nature of these
752 processes, and thus to understand the extent that Titan's surface may be chemically
753 interacting with its water-rich interior. Also of great importance to habitability are the
754 transient H₂O melt sheets and flows (e.g., Soderblom et al., 2010) associated with impacts.
755 On Titan, several features with volcanic landforms, lengthy flows, tall mountains, large

756 caldera-like depressions, have been identified as possible cryovolcanic sites but could also
757 possibly be due to other endogenic processes (Lopes et al., 2016; Solomonidou et al., 2016).
758 At present, the Hotei Regio flows and the Sotra Patera region, which includes Sotra Patera, an
759 elliptical deep depression on Titan, Mohini Fluctus, a lengthy flow feature, and Doom and
760 Erebor Montes, two volcanic edifices, are considered to host the strongest candidates for
761 cryovolcanism on Titan (Lopes et al., 2013; Solomonidou et al., 2014, 2016). E²T would
762 provide high resolution mapping (30 m/pixel with DTM vertical resolution of 10 m) of
763 regions that are candidates for cryovolcanic activity.

764 A variety of mountainous topography has been observed on Titan (Radebaugh et al., 2007;
765 Cook-Hallett et al., 2015). The observed morphologies of many of Titan's mountains suggest
766 contractional tectonism (Mitri et al., 2010; Liu et al., 2016). This is somewhat surprising,
767 however, since tectonic landforms observed on other ocean worlds and icy satellites in the
768 outer solar system appear to be extensional in nature. Understanding Titan's tectonic regime
769 would, thus not only provide insight into the transport of material between surface and the
770 interior, but also into the evolution of the other ocean worlds. We would test the hypothesis
771 that Titan's mountains are formed by contraction by mapping the faults driving mountain
772 formation in topographic context. The shape of the fault outcrop draped against topography
773 would allow us to measure the faults' dip, which would be ~30 degrees to the horizontal for
774 compressive mountains and ~60 degrees for extensional mountains.

775 In addition to cryovolcanism and tectonism, which may transport water to Titan's surface,
776 impact craters likely have created transient liquid-water environments on Titan's surface.
777 Because of Titan's dense atmosphere, models suggest that melt sheets and flows associated
778 with impact craters may remain liquid for 10⁴–10⁶ years (Thompson and Sagan, 1992;
779 Artemieva and Lunine, 2005), though the stability of such melts is questioned (Senft and

780 Stewart, 2011; Zahnle et al., 2014) and detailed imaging of the floors of young craters is
781 needed to constrain these models. Titan offers numerous pathways for interaction between its
782 organic-rich surface and liquid water. E²T would provide high-resolution mapping (30
783 m/pixel with DTM vertical resolution of 10 m) that would offer the ability to distinguish
784 cryovolcanic features and to investigate the morphology of Titan's mountains and impact
785 craters.

786

787 **4. Scientific Payload**

788 The Explorer of Enceladus and Titan (E²T) has a focused payload that would provide in-situ
789 mass spectrometry and high-resolution imaging of Enceladus' south polar terrain and plume,
790 and Titan's upper atmosphere and surface, from a solar-electric powered spacecraft in orbit
791 around Saturn. The in-situ measurements of Titan's upper atmosphere would be acquired
792 during 17 flybys with an altitude as low as 900 km. At Enceladus, in-situ measurements
793 would be conducted during 6 flythroughs of the plume and flybys of the south polar terrain at
794 altitudes between 50 and 150 km. At the closest approach the velocity of the S/C with respect
795 to Enceladus surface is ~5 km/s and with respect to Titan surface is ~7 km/s. Imaging data
796 will be collected during inbound and outbound segments of each flyby.

797 The E²T mission model payload consists of three science instruments: two time-of-flight
798 mass spectrometers (TOF-MS), the Ion and Neutral gas Mass Spectrometer (INMS) and the
799 Enceladus Icy Jet Analyzer (ENIJA); and a high-resolution infrared camera, Titan Imaging
800 and Geology, Enceladus Reconnaissance (TIGER). Two instruments in the E²T payload were
801 proposed to be provided by ESA member states, INMS, which would be provided by Swiss
802 Space Office (SSO) and ENIJA, which would be provided by German Aerospace Center
803 (DLR). NASA proposed to provide the third instrument, TIGER. The characteristics of the

804 science payload are shown in Table 2. In addition, a Radio Science Experiment (RSE), not
805 necessarily requiring specific hardware on-board the spacecraft – thus regarded as an
806 “experiment of opportunity”, was considered for further study. The RSE would improve the
807 current determination of the gravity fields of Enceladus and Titan, by using the radio links
808 between the E²T spacecraft and Earth to better constrain their internal structure. The
809 proposed main funding agency of the RSE is the Italian Space Agency (ASI).

810 TABLE 2

811 4.1 Ion and Neutral Mass Spectrometer (INMS)

812 The Ion and Neutral Mass Spectrometer (INMS) is a reflectron time-of-flight mass
813 spectrometer (TOF-MS) that would record mass spectra of neutral and ionised gases during
814 flybys and fly-throughs of Enceladus’ plume and Titan’s upper atmosphere. During flybys
815 and flythroughs of Saturn’s E-ring, Enceladus’ plume and of Titan’s upper atmosphere,
816 INMS will record mass spectra of neutral and positive and negative ionized gases within the
817 mass range 1 – 1000 u/e with a mass resolution at 5000 $m/\Delta m$ (50%) with a sensitivity
818 (detection threshold) of 1 cm^{-3} ($\sim 10^{-16}$ mbar) in a 5 s measurement cadence (Abplanalp et al.,
819 2010; Wurz et al., 2012). The Cassini INMS (Ion and Neutral Mass Spectrometer) is limited
820 to the detection of low mass species of 1–99 u and is therefore not able to measure the high-
821 mass molecular species abundant in Enceladus’ plume and in Titan’s upper atmosphere.
822 Further, E²T INMS’ high mass resolution ($m/\Delta m = 5000$), 50 times larger than Cassini
823 INMS, allows for the separation of isobaric interference such as occur at 16, 20, 28, and 40
824 u/e which is possible based on heritage of RTOF/ROSINA from the Rosetta mission (Scherer
825 et al., 2006; Wurz et al., 2015) as shown in Figure 5.

826 FIGURE 5

827 Cassini INMS only had the ability to measure positively charged ions. In-situ
828 measurements by the Cassini Plasma Spectrometer (CAPS) detected heavy negative ions in
829 Titan's ionosphere and negative water group ions in Enceladus' plume (Coates et al., 2010).
830 E²T INMS would record 10,000 mass spectra per second and accumulate these for a pre-set
831 period, allowing for a time resolution of measurements in the range from 0.1 to 300 s. The
832 maximum INMS resolution at Enceladus is 0.1 s (corresponding to a spatial resolution of
833 ~0.5 km for a S/C velocity of 5 km/s) to resolve small-scale structure in the plume; the
834 maximum used INMS resolution at Titan is 5 s (corresponding to a spatial resolution of ~35
835 km for a S/C velocity of 7 km/s).

836 The E²T INMS has heritage based on P-BACE instrument, on the Rosetta ROSINA and on
837 the gas-chromatograph-neutral gas mass spectrometer prototype which will be used in
838 upcoming lunar exploration conducted by the Russian Space Agency in 2019 (Hofer et al.,
839 2015;Wurz et al., 2015). Most recently, a similar instrument, the Neutral gas and Ion Mass
840 spectrometer (NIM) instrument of the Particle Environment Package (PEP) consortium, is
841 developed for the JUICE mission of ESA

842

843 **4.2 Enceladus Icy Jet Analyzer (ENIJA)**

844 Enceladus Icy Jet Analyzer (ENIJA) is optimized to search for prebiotic molecules and
845 biogenic compounds in objects with high dust fluxes and number densities such as occur in
846 Enceladus' plume or cometary comae. ENIJA consists of two time-of-flight mass
847 spectrometer (TOF-MS) subsystems and a software-enabled high flux detector (HFD) that
848 runs in parallel to the spectrometers. The HFD measurement mode will map the dynamical
849 profile (number density and size distribution) of Enceladus' ice jets. Compared to the Cassini
850 CDA (Cosmic Dust Analyzer), ENIJA has a 40 times better mass resolution, a 100 times

851 better maximum flux and sensitivity, and a spatial resolution that is 50 times better (Srama et
852 al., 2015). Moreover, the twin-detector instrument will acquire mass spectra of both cations
853 and anions created upon ice particle impact, simultaneously, whereas CDA only measured
854 cations. During flythroughs of Enceladus plume and in the E ring, ENIJA provides time-of-
855 flight mass spectra for ice particles with a mass range of 1-2000 u with a mass resolution
856 ($m/\Delta m$) of 970 between 23-2000 u. ENIJA acquires TOF mass spectra of individual ice
857 grains by impact ionization and analyses the generated anions and cations with two separate
858 time of flight spectrometer sub-units. In this way ENIJA is able to quantify organic
859 compounds at <10 ppm; additionally some polar organic species, such as most amino acids,
860 can be quantified well below 1 ppm (Figure 6). With a dynamic range up to 10^8 , inorganic
861 trace components with sub-ppm concentrations from Enceladus' ocean, can now be
862 investigated simultaneously with the more abundant mineral species. ENIJA is not a newly
863 developed instrument; rather it is an optimization and miniaturization of flight-proven
864 hardware. ENIJA has heritage based on Giotto-Particle Impact Analyzer (PIA), Stardust
865 Cometary Interstellar Dust Analyzer (CIDA), Cassini's' Cosmic Dust Analyzer (CDA),
866 Rosetta-COSIMA and Europa-SURface Dust mass Analyzer (SUDA).

867 FIGURE 6

868

869 **4.3 Titan Imaging and Geology, Enceladus Reconnaissance (TIGER)**

870 Titan Imaging and Geology, Enceladus Reconnaissance (TIGER) is a near infrared (NIR)
871 camera designed to acquire high resolution images of Titan and Enceladus. TIGER would
872 observe Titan at 30–100 m/pixel in three wavelengths, 1.3, 2, and 5 μm and Enceladus
873 emissions at 1 m/pixel at two wavelengths, 5 and 5.3 μm . Images acquired by TIGER would
874 enable investigation of Titan's geology, hydrology, and compositional variability and study

875 of the composition and kinematics of Enceladus' jets and plumes. The TIGER band passes
876 are selected to match with Titan's atmospheric transmission windows (Lemmon et al., 1993;
877 Sotin et al., 2005) to enable direct ground observations using reflected sunlight and to
878 measure thermal emission from Enceladus. The 5 μm images are subject to virtually no
879 scattering from Titan's atmospheric aerosols, allowing diffraction limited images achieving
880 spatial resolutions an order of magnitude better than Cassini observations (Clark et al., 2010;
881 Soderblom et al., 2012; Barnes et al., 2014) and would be highly sensitive to organic
882 composition (Clark et al., 2010; Barnes et al., 2014). TIGER has the capability to image Titan
883 at Huygens DISR resolution (Figure 7). At Enceladus, the 5 and 5.3 μm observations would
884 measure thermal emission of surfaces as cold as 130 K and would provide temperature maps
885 of the surface at Cassini-ISS image scales. A fine steering mirror (FSM) would be employed
886 to select and track regions of interest during the flyby and compensate for spacecraft jitter
887 allowing for longer exposures and better signal-to-noise ratio (SNR). Digital time-delay
888 integration (TDI) would also be employed, as needed, during closest approach when the
889 ground speed is highest.

890 **FIGURE 7**

891 While the TIGER instrument is a new design, it utilizes high-heritage subsystems (\geq TRL
892 6). The TIGER Focal Plane Array (FPA) is from Teledyne Imaging Sensors and utilizes the
893 same HgCdTe detector and H2RG qualified for James Webb Space Telescope (JWST) Near
894 Infrared Camera (NIRCam) (Reike et al., 2005), Near Infrared Spectrometer (NIRSpec)
895 (Rauscher et al., 2004), and Fine Guidance Sensor (FGS) (Doyon et al., 2012) instruments.
896 TIGER also implements FPA readout electronics that have been qualified extensively for the
897 JWST instruments (Loose et al., 2006) and are used by the Euclid Near Infrared Spectrometer
898 and Photometer (NISP) (Maciaszek et al., 2014).

900 **4.4 Radio Science Experiment**

901 Gravity field measurements are powerful tools to constrain the interior structure of the planets
902 and satellites and to assess mass anomalies, providing information on the internal dynamics
903 and evolution. The observable quantities used by gravity science experiments are obtained by
904 means of spacecraft tracking at microwave frequencies from a terrestrial ground antenna. The
905 eight gravity flybys of Titan conducted by the Cassini mission (not including the T122 flyby,
906 recently completed in August 2016) yielded sufficient information to obtain a robust
907 estimation of the degree-3 static gravity field, plus the fluid Love number k_2 (Iess et al.,
908 2010,2012); however, this was not the case for Enceladus (Rappaport et al., 2008; Iess et al.,
909 2014), where only the degree-2 static gravity field and J_3 were observed, and the tidal
910 response to Saturn's gravity was not detected.

911 In Enceladus' south polar terrain a larger time-variation of the gravity field with respect to
912 the global solution of the time variation of the gravity field is expected because the ice shell
913 thickness is anticipated to be locally thin in that area. A gravity science experiment, based on
914 radio tracking and precise spacecraft multiarc orbit determination (see e.g. Tortora et al.,
915 2016), would determine the local solution of the gravity field of Enceladus at the south polar
916 terrain thus allowing the determination of the thickness variation at the south polar regions
917 and constraining the mechanical properties (viscosity) of the ice overlying the outer ice shell.
918 The expected tidal deformation is characterized by a pattern more complex than the standard
919 degree-two pattern, with a strong amplification of the tidal fluctuation in the south polar
920 terrain (Brzobohaty et al., 2016).

921 For Titan gravity science, a desirable objective would be the improve of Cassini's results
922 in terms of reduction of the uncertainty in the fluid Love number k_2 . In particular, the

923 geophysics objectives relative to the subsurface liquid ocean extent, shell thickness and shell
924 viscosity would be improved if the formal uncertainty of k_2 could be reduced down to values
925 in the range 0.05-0.01. The feasibility of such result strongly depends on the actual geometry
926 of Titan's flyby (in particular: altitude at pericenter and mean anomaly of Titan around Saturn
927 at the time of closest approach with the E²T spacecraft), in addition to the stability of the
928 radio link (preferably at Ka-band, to reduce the detrimental effect of dispersive media).

929 The availability of a two-way (uplink and downlink) radio system would also allow
930 expanding the long series of Titan's occultations carried out by Cassini's radio science
931 subsystem to probe Titan's neutral and ionized atmosphere (Coustenis et al., 2016; Kliore et
932 al., 2008, 2011; Schinder et al., 2012, 2015). The main objective would be the
933 characterization of Titan's atmospheric structure (pressure, density, and total electron content
934 profiles, versus altitude) at different latitude/longitudes.

935

936 **5. Proposed Mission and Spacecraft Configuration**

937 The baseline scenario for the E²T mission is a solar electric powered spacecraft (S/C), in orbit
938 around Saturn, performing multiple flybys of Titan and Enceladus. The baseline includes a
939 shared launch on the Ariane 6.4 with a co-manifest of estimated launch mass of ~2636 kg to
940 geosynchronous transfer orbit (GTO), with a forecasted shared launch opportunity in 2030.
941 The Ariane 6.4 with four solid rocket boosters is scheduled to debut in 2020–2021. The upper
942 stage reignition capability of the Ariane 6.4 will enable a GTO/escape dual launch. The mass
943 estimate for the co-manifest places it in the lower end of the Intermediate Class (2,500-4,200
944 kg) of commercial satellites (FAA, 2015). After a transfer from GTO to a hyperbolic escape
945 trajectory, E²T S/C would pursue a gravity assist flyby of the Earth to help propel itself to the
946 Saturn system. The cruise phase from Earth to Saturn would be 6 years long. The E²T tour in

947 the Saturn system would be 3.5 years long. The E²T tour consists of 6 flybys of Enceladus
948 above the south polar terrain with a flight altitude range between 50 to 150 km, and 17 flybys
949 of Titan at a reference flight altitude ranging from 1500 down to 900 km.

950

951 **5.1 Transfer Orbit to Saturn**

952 The nominal transfer to Saturn uses a 1:1⁺ resonant Earth flyby trajectory, as shown in Table
953 3 and Figure 8. Electric propulsion is used to strongly increase the hyperbolic flyby speed at
954 the Earth, and to provide a subsequent energy boost to reduce the total flight time to 6 years
955 to Saturn orbit insertion (SOI). After separation from the co-manifested satellite and the
956 SYLDA carrier, the upper stage will be re-ignited near perigee to impart approximately 1.2
957 km/s ΔV to the E²T S/C, putting it on a hyperbolic escape trajectory with a C₃ of 9.6 km²/s².
958 Thanks to the use of electric propulsion and an Earth gravity assist, the declination of the
959 asymptote can vary between ± 5 degrees without significant propellant mass penalty.
960 Similarly, as shown in Table 4, there is negligible performance variation over a 21-day launch
961 period. The data in Table 3 is based on a proposed launch from January-May 2030 during
962 which there is little variation in flight time or required propellant mass. Lunar flybys on the
963 escape trajectory were not considered, but could be used to effectively lower the required
964 escape ΔV which in turn would allow for a heavier co-manifested satellite.

965

FIGURE 8

966

TABLE 3

967

FIGURE 9

968

TABLE 4

969

970 **5.2 Saturn Tour**

971 The duration of the tour from SOI through to the end of the 17-flyby Titan phase is about 3.5
972 years. A sample tour is shown in Figure 9. Like Cassini, end-of-mission spacecraft disposal is
973 Saturn impact, by means of three to four additional Titan flybys.

974 The tour is divided in a first Enceladus science phase and in a second Titan science phase.
975 The S/C should perform at least 6 flybys of Enceladus above the south polar terrain and at
976 least 17 flybys of Titan. To prevent contamination from Titan's organics for Enceladus
977 science, E²T S/C will perform close flybys of Enceladus at the beginning of the tour
978 (Enceladus science phase); distant flybys of Titan will be performed during the initial tour
979 phase. After the main Enceladus phase, close flybys of Titan with atmospheric sampling will
980 be performed (Titan science phase).

981 **FIGURE 9**

982 During Enceladus science phase, E²T will provide in-situ sampling of the plume at a
983 minimum altitude from Enceladus' surface ranging between 50 and 150 km using INMS and
984 ENIJA. At the closest approach, the velocity of the S/C with respect to Enceladus' surface
985 will be approximately 5 km/s. E²T will provide high-resolution imaging of Enceladus surface
986 with the TIGER camera. During Enceladus flybys the observations of INMS, ENIJA and
987 TIGER will be performed simultaneously. During this phase observations of Titan's surface
988 using TIGER are scheduled during distant flybys.

989 During the Titan science phase, E²T will provide in-situ sampling of the upper atmosphere
990 at a minimum altitude from Titan surface as low as 900 km using INMS. At the closest
991 approach the velocity of the S/C with respect to Titan's surface will be approximately 7 km/s.

992 E²T will provide high-resolution imaging of Titan’s surface with TIGER camera. During
993 Titan flybys the observations of INMS and TIGER can be performed simultaneously.

994

995 **5.3 Spacecraft Design and Structure**

996 The proposed E²T spacecraft (S/C) design is the result of the harmonisation of several high-
997 TRL key space technologies already developed on behalf of several ESA space exploration
998 missions, such as: ExoMars 2016, JUICE, BepiColombo and Rosetta. The proposed E²T
999 spacecraft architecture would be derived from the ESA ExoMars Trace Gas Orbiter (TGO)
1000 developed for the 2016 mission. The proposed E²T architecture is in compliance with the
1001 Ariane 6.4 launcher size constraints. Table 5 summarizes its main technical characteristics.
1002 The E²T spacecraft baseline configuration is depicted in Figure 10.

1003 TABLE 5

1004 FIGURE 10

1005 The Solar Arrays (SA) are the main S/C electrical power source, whereas the S/C main
1006 battery provides the emergency backup one. The E²T four panel solar arrays are based on
1007 space-qualified Thales Alenia Space SolarBus W51 technologies and GaAs/Ge Low Intensity
1008 Low Temperature (LILT) solar cells technology used in the ESA JUICE mission. The Solar
1009 Electric Propulsion System (SEPS) is based on four (3+1 for redundancy) QinetiQ’s T6
1010 gridded ion thruster engines, whereas two chemical propulsion systems have been also
1011 implemented for S/C manoeuvres and Attitude and Orbital Control System (AOCS) purposes.
1012 The propulsion systems’ designs have been directly derived from different mission heritages,
1013 such as the two ESA missions GOCE and BepiColombo, and the NASA/ESA/ASI Cassini
1014 mission. The heritage of systems and subsystems from previous ESA missions requiring

1015 limited technological development enables a relatively low cost for the industrial
1016 development. The E²T S/C design was performed by Thales Alenia Space (TAS-I, Torino,
1017 Italy)

1018

1019 **6. Summary**

1020 E²T was proposed as mission led by ESA in collaboration with NASA and several ESA
1021 member states for the payload in response to ESA's M5 Cosmic Vision Call. The joint
1022 exploration of Enceladus and Titan with a flyby mission such as the E²T mission can address
1023 fundamental scientific questions regarding extra-terrestrial habitability, abiotic/prebiotic
1024 chemistry, the emergence of life, and the origin and evolution of ocean worlds. In the Solar
1025 System, the best candidates for habitability at present are the ocean worlds in the outer Solar
1026 System: Europa, Enceladus and Titan. Of these, only Enceladus and Titan provide
1027 environments that can be easily sampled from orbit in a single mission. Titan, with its
1028 organically rich and dynamic atmosphere and geology, and Enceladus, with its active plume
1029 composed of multiple jets, both harbouring subsurface oceans, are ideal environments in
1030 which to investigate the conditions for the emergence of life and the habitability of ocean
1031 worlds as well as the origin and evolution of complex planetary systems. The joint
1032 exploration of these two fascinating objects will allow us to better understand the origin of
1033 their organic-rich environment and will give access to planetary processes that have long
1034 been thought unique to the Earth.

1035 Given that the E²T mission concept proposes the first solar-powered mission beyond
1036 Jupiter, a four-point strategy to minimize the cost and meet the M5 criteria was used: 1) the
1037 reusing of systems and subsystems with a TRL ≥ 5 from previous ESA missions with a
1038 limited technological development necessary; 2) a science payload with a TRL ≥ 5 with low

1039 total mass (57.7kg), power (83.2 W) and data rate (115 Mbit/day) requirements; 3) a cruise
1040 phase with a duration of 6 years and a nominal mission operation duration of 3.5 years; and 4)
1041 a forecasted shared launch opportunity in 2030 with a commercial satellite to GTO by the
1042 Ariane 6.4 which will allow E²T to pursue a cost-effective launch that will enable an efficient
1043 Earth escape trajectory to the Saturn system. The E²T mission concept offers a cost-effective
1044 way to investigate the evolution and habitability of ocean worlds in the Saturn system and
1045 address key questions, which remain unanswered as the end of the Cassini-Huygens' mission
1046 draws near, regarding the origin, evolution and habitability of these ocean worlds. In
1047 combination with the results expected from the ESA JUICE mission on the ocean worlds
1048 around Jupiter, this mission would offer a unique opportunity to understand the habitable
1049 conditions in our own Solar System and beyond.

1050

1051

1052 **REFERENCES**

- 1053 Abplanalp et al. 2010. An optimised compact electron impact ion storage source for a time-
1054 of-flight mass spectrometer *International Journal of Mass Spectrometry* 294, 33-39.
- 1055 Aharonson, O., Hayes, A.G., Lunine, J.I., Lorenz, R.D., Allison, M.D., Elachi, C. 2009. An
1056 asymmetric distribution of lakes on Titan as a possible consequence of orbital forcing. *Nature*
1057 *Geoscience* 2, 851-854.
- 1058 Altwegg, K., H. Balsiger, A. Bar-Nun, J.-J. Berthelier, A. Bieler, P. Bochslers, C. Briois, U.
1059 Calmonte, M. Combi, H. Cottin, J. De Keyser, B. Fiethe, S.A. Fuselier, S. Gasc, T.I.
1060 Gombosi, K.C. Hansen, M. Hässig, A. Jäckel, E. Kopp, A. Korth, L. Le Roy, U. Mall, B.
1061 Marty, O. Mousis, T. Owen, H. Rème, M. Rubin, T. Sémon, C.-Y. Tzou, J.H. Waite, and P.
1062 Wurz, Prebiotic chemicals - amino acid and phosphorus - in the coma of comet
1063 67P/Churyumov-Gerasimenko, *Science Advances* 2:e1600285 (2016) 5pp, DOI:
1064 10.1126/sciadv.1600285
- 1065 Artemieva, N., Lunine, J.I. 2005. Impact cratering on Titan II. Global melt, escaping ejecta,
1066 and aqueous alteration of surface organics. *Icarus* 175, 522-533.
- 1067 Atreya, S.K., Adams, E.Y., Niemann, H.B., Demick-Montelara, J.E., Owen, T.C.,
1068 Fulchignoni, M., Ferri, F., Wilson, E.H. 2006. Titan's methane cycle. *Planetary and Space*
1069 *Science* 54, 1177-1187.
- 1070 Balsiger, H., and 49 colleagues 2007. Rosina Rosetta Orbiter Spectrometer for Ion and
1071 Neutral Analysis. *Space Science Reviews* 128, 745-801.
- 1072 Barnes, J.W., Sotin, C., Soderblom, J.M., Brown, R.H., Hayes, A.G., Donelan, M.,
1073 Rodriguez, S., Le Mouélic, S., Baines, K.H. and McCord, T.B., 2014. Cassini/VIMS observes
1074 rough surfaces on Titan's Punga Mare in specular reflection. *Planetary Science*, 3(1), p.1.
- 1075 Barnes, J., et al., AVIATR—Aerial Vehicle for In-Situ and Airborne Titan Reconnaissance,
1076 *Experimental Astronomy*, Vol. 33, No. 1, 2012, pp. 55–127. doi:10.1007/s10686-011-9275-9
- 1077 Beghin, C., Randriamboarison, O., Hamelin, M., Karkoschka, E., Sotin, C., Whitten, R.C.,
1078 Berthelier, J.J., Grard, R., Simoes, F. 2012. Analytic theory of Titan's Schumann resonance:
1079 Constraints on ionospheric conductivity and buried water ocean. *Icarus* 218, 1028-1042.
- 1080 Beletic, J.W., Blank, R., Gulbransen, D., Lee, D., Loose, M., Piquette, E.C., Sprafke, T.,
1081 Tennant, W.E., Zandian, M. and Zino, J., 2008, August. Teledyne Imaging Sensors: infrared
1082 imaging technologies for astronomy and civil space. In *SPIE Astronomical Telescopes+*
1083 *Instrumentation* (pp. 70210H-70210H). International Society for Optics and Photonics.
- 1084 Bell, J.F., Squyres, S.W., Herkenhoff, K.E., Maki, J.N., Arneson, H.M., Brown, D., Collins,
1085 S.A., Dingizian, A., Elliot, S.T., Hagerott, E.C. and Hayes, A.G., 2003. Mars exploration
1086 rover Athena panoramic camera (Pancam) investigation. *Journal of Geophysical Research:*
1087 *Planets*, 108(E12).

- 1088 Bèzard, B. 2014. The methane mole fraction in Titan's stratosphere from DISR
1089 measurements during the Huygens probe's descent. *Icarus* 242, 64-73.
- 1090 Birch, S., and 20 colleagues 2016. Geomorphologic Mapping of Titan's Polar Terrains:
1091 Constraining Surface Processes and Landscape Evolution. *Icarus*, in press.
- 1092 Blank, R., Anglin, S., Beletic, J.W., Bhargava, S., Bradley, R., Cabelli, C.A., Chen, J.,
1093 Cooper, D., Demers, R., Eads, M. and Farris, M., 2012, September. H2RG focal plane array
1094 and camera performance update. In *SPIE Astronomical Telescopes+ Instrumentation* (pp.
1095 845310-845310). International Society for Optics and Photonics.
- 1096 Brown, M.E., Smith, A.L., Chen, C., Adamkovics, M. 2009. Discovery of Fog at the South
1097 Pole of Titan. *The Astrophysical Journal* 706, L110-L113.
- 1098 Brown, R.H., Baines, K.H., Bellucci, G., Bibring, J.P., Buratti, B.J., Capaccioni, F., Ceroni,
1099 P., Clark, R.N., Coradini, A., Cruikshank, D.P. and Drossart, P., 2004. The Cassini visual and
1100 infrared mapping spectrometer (VIMS) investigation. In *The Cassini-Huygens Mission* (pp.
1101 111-168). Springer Netherlands.
- 1102 Brzobohaty, T., Ferfecki, P., Kozubek, T., Markopoulos, A., Behoukova, M., Tobie, G.,
1103 Choblet, G., Cadek, O. 2016. Effect of ice-shell thickness variations on the tidal response of
1104 Saturn's moon Enceladus, *Icarus*, in revision.
- 1105 Burr, D.M., Emery, J.P., Lorenz, R.D., Collins, G.C., Carling, P.A. 2006. Sediment transport
1106 by liquid surficial flow: Application to Titan. *Icarus* 181, 235-242.
- 1107 Burr, D.M., Drummond, S.A., Cartwright, R., Black, B.A., Perron, J.T. 2013. Morphology of
1108 fluvial networks on Titan: Evidence for structural control. *Icarus* 226, 742-759.
- 1109 Čadek, O., and 10 colleagues 2016. Enceladus's internal ocean and ice shell constrained from
1110 Cassini gravity, shape, and libration data. *Geophysical Research Letters* 43, 5653-5660.
- 1111 Canup, R.M. 2010. Origin of Saturn's rings and inner moons by mass removal from a lost
1112 Titan-sized satellite. *Nature* 468, 943-946.
- 1113 Charnoz, S., Crida, A., Castillo-Rogez, J.C., Lainey, V., Dones, L., Karatekin, O., Tobie, G.,
1114 Mathis, S., Le Poncin-Lafitte, C., Salmon, J. 2011. Accretion of Saturn's mid-sized moons
1115 during the viscous spreading of young massive rings: Solving the paradox of silicate-poor
1116 rings versus silicate-rich moons. *Icarus* 216, 535-550.
- 1117 Clark, R.N., Curchin, J.M., Barnes, J.W., Jaumann, R., Soderblom, L., Cruikshank, D.P.,
1118 Brown, R.H., Rodriguez, S., Lunine, J., Stephan, K. and Hoefen, T.M., 2010. Detection and
1119 mapping of hydrocarbon deposits on Titan. *Journal of Geophysical Research: Planets*,
1120 115(E10).
- 1121 Coates, A.J., Crary, F.J., Lewis, G.R., Young, D.T., Waite, J.H., Sittler, E.C. 2007. Discovery
1122 of heavy negative ions in Titan's ionosphere. *Geophysical Research Letters* 34, L22103.

- 1123 Coates, A.J., Jones, G.H., Lewis, G.R., Wellbrock, A., Young, D.T., Crary, F.J., Johnson,
1124 R.E., Cassidy, T.A., Hill, T.W. 2010. Negative ions in the Enceladus plume. *Icarus* 206, 618-
1125 622.
- 1126 Cook-Hallett, C., Barnes, J.W., Kattenhorn, S.A., Hurford, T., Radebaugh, J., Stiles, B.,
1127 Beuthe, M. 2015. Global contraction/expansion and polar lithospheric thinning on Titan from
1128 patterns of tectonism. *Journal of Geophysical Research (Planets)* 120, 1220-1236.
- 1129 Cordier, D., Mousis, O., Lunine, J.I., Lebonnois, S., Lavvas, P., Lobo, L.Q., Ferreira, A.G.M.
1130 2010. About the Possible Role of Hydrocarbon Lakes in the Origin of Titan's Noble Gas
1131 Atmospheric Depletion. *The Astrophysical Journal* 721, L117-L120.
- 1132 Cornet, T., Cordier, D., Bahers, T.L., Bourgeois, O., Fleurant, C., Mouelic, S.L., Altobelli, N.
1133 2015. Dissolution on Titan and on Earth: Toward the age of Titan's karstic landscapes.
1134 *Journal of Geophysical Research (Planets)* 120, 1044-1074.
- 1135 Coustenis, A. and 114 co-authors, TanDEM: Titan and Enceladus Mission, *Experimental*
1136 *Astronomy*, 23, 893-946, 2009
- 1137 Coustenis, A., Lunine, J., Lebreton, J.-P., Matson, D., Erd, Ch., Reh, K., Beauchamp, P.,
1138 Lorenz, R., Waite, H., Sotin, Ch., Gurvits, L., Hirtzig, M., 2009. Earth-based support for the
1139 Titan Saturn Mission. *Earth Moon and Planets* 105, 135-142, DOI: 10.1007/s11038-009-
1140 9308-9.
- 1141 Coustenis, A., Bampasidis, G., Achterbergh, R. K., Lavvas, P., Nixon, C. A., Jennings, D. E.,
1142 Teanby, N. A., Vinatier, S., Flasar, F. M., Carlson, R. C., Orton, G., Romani, P. N.,
1143 Guardique, E. A., 2013. Evolution of the stratospheric temperature and chemical composition
1144 over one Titanian year. *Astrophys. J.* 799, 177, 9p.
- 1145 Coustenis, A., Jennings, D. E., Achterbergh, R. K., Bampasidis, G., Lavvas, P., Nixon, C. A.,
1146 Teanby, N. A., Anderson, C. M., Flasar, F. M., 2016. Titan's temporal evolution in
1147 stratospheric trace gases near the poles. *Icarus* 270, 409-420.
- 1148 Crary, F.J., Magee, B.A., Mandt, K., Waite, J.H., Westlake, J., Young, D.T. 2009. Heavy
1149 ions, temperatures and winds in Titan's ionosphere: Combined Cassini CAPS and INMS
1150 observations. *Planetary and Space Science* 57, 1847-1856.
- 1151 Davies, A.G., Sotin, C., Choukroun, M., Matson, D.L., Johnson, T.V. 2016. Cryolava flow
1152 destabilization of crustal methane clathrate hydrate on Titan. *Icarus* 274, 23-32.
- 1153 Dorn, E.D., Adami, C. 2011. Robust Monomer-Distribution Biosignatures in Evolving
1154 Digital Biota. *Astrobiology* 11, 959-968.
- 1155 Dougherty, M.K., Khurana, K.K., Neubauer, F.M., Russell, C.T., Saur, J., Leisner, J.S.,
1156 Burton, M.E. 2006. Identification of a Dynamic Atmosphere at Enceladus with the Cassini
1157 Magnetometer. *Science* 311, 1406-1409.

- 1158 Doyon, R., Hutchings, J., Beaulieu, M., Albert, L., Lafrenière, D., Willott, C., Touahri, D.,
1159 Rowlands, N., Maszkiewicz, M., Fullerton, A.W. and Volk, K. 2012. The JWST fine
1160 guidance sensor (FGS) and near-infrared imager and slitless spectrograph (NIRISS). In Proc.
1161 SPIE (Vol. 8442, p. 84422R).
- 1162 Eldering, A., Kaki, S. and Bennett, M.W., 2014, December. The Orbiting Carbon
1163 Observatory-3 (OCO-3) mission: An overview. In AGU Fall Meeting Abstracts (Vol. 1, p.
1164 04).
- 1165 Elsila, J.E., Glavin, D.P., Dworkin, J.P. 2009. Cometary glycine detected in samples returned
1166 by Stardust. *Meteoritics and Planetary Science* 44, 1323-1330.
- 1167
1168 Estrada, P.R., Mosqueira, I., Lissauer, J.J., D'Angelo, G., Cruikshank, D.P. 2009. Formation
1169 of Jupiter and Conditions for Accretion of the Galilean Satellites. *Europa*, Edited by Robert
1170 T. Pappalardo, William B. McKinnon, Krishan K. Khurana ; with the assistance of R. Dotson
1171 with 85 collaborating authors. University of Arizona Press, Tucson, 2009. The University of
1172 Arizona space science series ISBN: 9780816528448, p.27 27.
- 1173 Federal Aviation Administration (FAA) Commercial Space Transportation (AST) and the
1174 Commercial Space Transportation Advisory Committee (COMSTAC) 2015 Commercial
1175 Space Transportation Forecast April 2015
- 1176 Fulchignoni, M., and 42 colleagues 2005. In situ measurements of the physical characteristics
1177 of Titan's environment. *Nature* 438, 785-791.
- 1178 Gudipati, M. S., Jacovi, R., Couturier-Tamburelli, I., Lignell, A., Allen, M. 2013.
1179 Photochemical activity of Titan's low-altitude condensed haze. *Nature Communications*.
1180 4:1648, DOI: 10.1038/ncomms2649.
- 1181 Glein, C.R., Zolotov, M.Y., Shock, E.L. 2008. The oxidation state of hydrothermal systems
1182 on early Enceladus. *Icarus* 197, 157-163.
- 1183 Glein, C.R., Baross, J.A., Waite, J.H. 2015. The pH of Enceladus' ocean. *Geochimica et*
1184 *Cosmochimica Acta* 162, 202-219.
- 1185 Goguen, J.D., and 12 colleagues 2013. The temperature and width of an active fissure on
1186 Enceladus measured with Cassini VIMS during the 14 April 2012 South Pole flyover. *Icarus*
1187 226, 1128-1137.
- 1188 Griffith, C.A., Zahnle, K. 1995. Influx of cometary volatiles to planetary moons: The
1189 atmospheres of 1000 possible Titans. *Journal of Geophysical Research* 100, 16907-16922.
- 1190 Griffith, C.A., Mitchell, J.L., Lavvas, P., Tobie, G. 2013. Titan's Evolving Climate.
1191 *Comparative Climatology of Terrestrial Planets* 91-119.
- 1192 Hansen, C.J., Esposito, L., Stewart, A.I.F., Colwell, J., Hendrix, A., Pryor, W., Shemansky,
1193 D., West, R. 2006. Enceladus' Water Vapor Plume. *Science* 311, 1422-1425.

- 1194 Hansen, C.J., Esposito, L.W., Stewart, A.I.F., Meinke, B., Wallis, B., Colwell, J.E., Hendrix,
1195 A.R., Larsen, K., Pryor, W., Tian, F. 2008. Water vapour jets inside the plume of gas leaving
1196 Enceladus. *Nature* 456, 477-479.
- 1197 Hansen, C.J., and 10 colleagues 2011. The composition and structure of the Enceladus plume.
1198 *Geophysical Research Letters* 38, L11202.
- 1199 Hayes, A., and 13 colleagues 2008. Hydrocarbon lakes on Titan: Distribution and interaction
1200 with a porous regolith. *Geophysical Research Letters* 35, L09204.
- 1201 Hayes, A.G., and 11 colleagues 2010. Bathymetry and absorptivity of Titan's Ontario Lacus.
1202 *Journal of Geophysical Research (Planets)* 115, E09009.
- 1203 Hayes, A.G., and 14 colleagues 2011. Transient surface liquid in Titan's polar regions from
1204 Cassini. *Icarus* 211, 655-671.
- 1205 Hässig, M., Altwegg, K., Balsiger, H., Berthelier, J.J., Calmonte, U., Combi, M., De Keyser,
1206 J., Fiethe, B., Fuselier, S.A., Rubin, M. 2013. ROSINA/DFMS capabilities to measure
1207 isotopic ratios in water at comet 67P/Churyumov-Gerasimenko. *Planetary and Space Science*
1208 84, 148-152.
- 1209 Hedman, M.M., Nicholson, P.D., Showalter, M.R., Brown, R.H., Buratti, B.J., Clark, R.N.
1210 2009. Spectral Observations of the Enceladus Plume with Cassini-Vims. *The Astrophysical*
1211 *Journal* 693, 1749-1762.
- 1212 Hofer, L., and 10 colleagues 2015. Prototype of the gas chromatograph-mass spectrometer to
1213 investigate volatile species in the lunar soil for the Luna-Resurs mission. *Planetary and Space*
1214 *Science* 111, 126-133.
- 1215
1216 Hörst, S.M., Vuitton, V., Yelle, R.V. 2008. Origin of oxygen species in Titan's atmosphere.
1217 *Journal of Geophysical Research (Planets)* 113, E10006.
- 1218 Hörst, S.M., and 12 colleagues 2012. Formation of Amino Acids and Nucleotide Bases in a
1219 Titan Atmosphere Simulation Experiment. *Astrobiology* 12, 809-817.
- 1220 Howett, C.J.A., Spencer, J.R., Pearl, J., Segura, M. 2011. High heat flow from Enceladus'
1221 south polar region measured using 10-600 cm⁻¹ Cassini/CIRS data. *Journal of Geophysical*
1222 *Research (Planets)* 116, E03003.
- 1223 Hsu, H.-W., Postberg, F., Kempf, S., Trieloff, M., Burton, M., Roy, M., Moragas-
1224 Klostermeyer, G., Srama, R. 2011. Stream particles as the probe of the dust-plasma-
1225 magnetosphere interaction at Saturn. *Journal of Geophysical Research (Space Physics)* 116,
1226 A09215.
- 1227 Hsu, H.-W., Postberg, F., Sekine, Y., Kempf, S., Horanyi, M., Juhasz, A., Srama, R. 2014.
1228 Silica Nanoparticles Provide Evidence for Hydrothermal Activities at Enceladus. *Workshop*
1229 *on the Habitability of Icy Worlds* 1774, 4042.

- 1230 Hsu, H.-W., and 14 colleagues 2015. Ongoing hydrothermal activities within Enceladus.
1231 Nature 519, 207-210.
- 1232 Hurford, T.A., Bills, B.G., Helfenstein, P., Greenberg, R., Hoppa, G.V., Hamilton, D.P. 2009.
1233 Geological implications of a physical libration on Enceladus. Icarus 203, 541-552.
- 1234 Iess, L., Rappaport, N.J., Jacobson, R.A., Racioppa, P., Stevenson, D.J., Tortora, P.,
1235 Armstrong, J.W., Asmar, S.W. 2010. Gravity Field, Shape, and Moment of Inertia of Titan.
1236 Science 327, 1367.
- 1237 Iess, L., Jacobson, R.A., Ducci, M., Stevenson, D.J., Lunine, J.I., Armstrong, J.W., Asmar,
1238 S.W., Racioppa, P., Rappaport, N.J., Tortora, P. 2012. The Tides of Titan. Science 337, 457.
- 1239 Iess, L., and 10 colleagues 2014. The Gravity Field and Interior Structure of Enceladus.
1240 Science 344, 78-80.
- 1241 Ingersoll, A.P., Pankine, A.A. 2010. Subsurface heat transfer on Enceladus: Conditions under
1242 which melting occurs. Icarus 206, 594-607.
- 1243 Ingersoll, A.P., Ewald, S.P. 2011. Total particulate mass in Enceladus plumes and mass of
1244 Saturn's E ring inferred from Cassini ISS images. Icarus 216, 492-506.
- 1245 Ives, D., Finger, G., Dorn, R., Eschbaumer, S., Mehrgan, L., Meyer, M. and Stegmeier, J.,
1246 2010, July. Performance evaluation of 5 μm cut-off Hawaii-2RG detectors using the fast
1247 readout amplifiers. In SPIE Astronomical Telescopes+ Instrumentation (pp. 77421S-77421S).
1248 International Society for Optics and Photonics.
- 1249 Jennings, D.E., Romani, P.N., Bjoraker, G.L., Sada, P.V., Nixon, C.A., Lunsford, A.W.,
1250 Boyle, R.J., Hesman, B.E., McCabe, G.H. 2009. 12C/13C Ratio in Ethane on Titan and
1251 Implications for Methane's Replenishment. Journal of Physical Chemistry A 113, 11101-
1252 11106.
- 1253 Johnson, W.R.; Hook, S.J. 2016. Mid and thermal infrared remote sensing at the Jet
1254 Propulsion Laboratory. Proc SPIE (Vol. 9819, p. 98190H).
- 1255 Kempf, S., and 11 colleagues 2005. Composition of Saturnian Stream Particles. Science 307,
1256 1274-1276.
- 1257 Kiely, A. and Klimesh M., 2003. The ICER Progressive Wavelet Image Compressor, IPN
1258 Progr. Rep. 42-155, Jet Propuls. Lab., Pasadena, Calif.
- 1259 Kite, E.S., Rubin, A.M. 2016. Sustained eruptions on Enceladus explained by turbulent
1260 dissipation in tiger stripes. Proceedings of the National Academy of Science 113, 3972-3975.
- 1261 Klimesh, M., Stanton, V. and Watola D., 2001. Hardware Implementation of a lossless image
1262 compression algorithm using a field programmable gate array, TMO Progr. Rep. 42-144,
1263 October -December 2000, pp. 1 -11, Jet Propuls. Lab., Pasadena, Calif.

- 1264 Kliore, A.J., Nagy, A.F., Cravens, T.E., Richard, M.S., Rymer, A.M. 2011. Unusual electron
 1265 density profiles observed by Cassini radio occultations in Titan's ionosphere: Effects of
 1266 enhanced magnetospheric electron precipitation? *Journal of Geophysical Research: Space*
 1267 *Physics*, 116, A11318.
- 1268 Kliore, A.J. et al. 2008. First results from the Cassini radio occultations of the Titan
 1269 ionosphere. *Journal of Geophysical Research: Space Physics* 113 (9), A09317
- 1270 Lainey, V., and 10 colleagues 2012. Strong Tidal Dissipation in Saturn and Constraints on
 1271 Enceladus' Thermal State from Astrometry. *The Astrophysical Journal* 752, 14.
- 1272 Lainey, V. 2016. Quantification of tidal parameters from Solar System data. *Celestial*
 1273 *Mechanics and Dynamical Astronomy* .
- 1274 Lavvas, P., Yelle, R. V., Koskinen, T., Bazin, A., Vuitton, V., Vigren, E., Galand, M.,
 1275 Wellbrocke, A., Coates, A. J., Wahlund, J.-E., Crary, F. J., Snowden, D. 2013. Aerosol
 1276 growth in Titan's ionosphere, *PNAS*, 110(8), 2729-2734.
- 1277 Leary, J., Jones, C., Lorenz, R., Strain, R. D., and Waite, J. H., Titan Explorer Flagship
 1278 Mission Study, Johns Hopkins Univ., Applied Physics Lab., Laurel, MD, Aug. 2007; also
 1279 http://www.lpi.usra.edu/opag/Titan_Explorer_Public_Report.pdf, Jan. 2008 [retrieved 2015].
- 1280 Lemmon, M.T., Karkoschka, E. and Tomasko, M., 1993, Titan's Rotation: Surface Features
 1281 Observed. *Icarus*, 103, pp. 329-332.
- 1282 Liu, Z.Y.C., Radebaugh, J., Harris, R.A., Christiansen, E.H., Neish, C.D., Kirk, R.L., Lorenz,
 1283 R.D. 2016. The tectonics of Titan: Global structural mapping from Cassini RADAR. *Icarus*
 1284 270, 14-29.
- 1285 Loose, M., Beletic, J., Garnett, J. and Muradian, N., 2006, June. Space qualification and
 1286 performance results of the SIDECAR ASIC. In *SPIE Astronomical Telescopes+*
 1287 *Instrumentation* (pp. 62652J-62652J). International Society for Optics and Photonics.
- 1288 Lopes, R.M.C., and 43 colleagues 2007. Cryovolcanic features on Titan's surface as revealed
 1289 by the Cassini Titan Radar Mapper. *Icarus* 186, 395-412.
- 1290 Lopes, R.M.C., and 15 colleagues 2013. Cryovolcanism on Titan: New results from Cassini
 1291 RADAR and VIMS. *Journal of Geophysical Research (Planets)* 118, 416-435.
- 1292 Lopes, R.M.C., Malaska, M.J., Solomonidou, A., LeGall, A., Janssen, M.A., Neish, C.,
 1293 Turtle, E.P., Birch, S.P.D., Hayes, A.G., Radebaugh, J., Coustenis, A., Schoenfeld, A., Stiles,
 1294 B.W., Kirk, R.L., Mitchell, K.L., Stofan, E.R., Lawrence, K.J., and the Cassini RADAR
 1295 Team (2016). Nature, Distribution, and Origin of Titan's Undifferentiated Plains
 1296 ("Blandlands"). *Icarus*, 270, 162-182.
- 1297 Lorenz, R.D., and 39 colleagues 2006. The Sand Seas of Titan: Cassini RADAR
 1298 Observations of Longitudinal Dunes. *Science* 312, 724-727.

- 1299 Lorenz, R. D., Post-Cassini Exploration of Titan: Science Rationale and Mission Concepts,
1300 Journal of the British Interplanetary Society, Vol. 53, 2000, pp. 218–234.
- 1301 Lorenz, R. D. A Review of Titan Mission Studies, Journal of the British Interplanetary
1302 Society, 62, 162-174, 2009
- 1303 Lunine, J.I., Stevenson, D.J. 1982. Formation of the Galilean satellites in a gaseous nebula.
1304 Icarus 52, 14-39.
- 1305 Lunine, J.I., Stevenson, D.J. 1987. Clathrate and ammonia hydrates at high pressure -
1306 Application to the origin of methane on Titan. Icarus 70, 61-77.
- 1307 Lunine, J., Choukroun, M., Stevenson, D., Tobie, G. 2010. The Origin and Evolution of
1308 Titan. Titan from Cassini-Huygens 35.
- 1309 Maciaszek, T., Ealet, A., Jahnke, K., Prieto, E., Barbier, R., Mellier, Y., Costille, A., Ducret,
1310 F., Fabron, C., Gimenez, J.L. and Grange, R., 2014, August. Euclid near infrared
1311 spectrophotometer instrument concept and first test results at the end of phase B. In SPIE
1312 Astronomical Telescopes+ Instrumentation (pp. 91430K-91430K). International Society for
1313 Optics and Photonics.
- 1314 MacKenzie, S.M., and 10 colleagues 2014. Evidence of Titan's climate history from evaporite
1315 distribution. Icarus 243, 191-207.
- 1316 Malaska, M.J., Lopes, R.M., Hayes, A.G., Radebaugh, J., Lorenz, R.D., Turtle, E.P. 2016.
1317 Material transport map of Titan: The fate of dunes. Icarus 270, 183-196.
- 1318 Mandt, K.E., and 18 colleagues 2012. Ion densities and composition of Titan's upper
1319 atmosphere derived from the Cassini Ion Neutral Mass Spectrometer: Analysis methods and
1320 comparison of measured ion densities to photochemical model simulations. Journal of
1321 Geophysical Research (Planets) 117, E10006.
- 1322 McKay, C.P., Porco, C., Altheide, T., Davis, W.L., Kral, T.A. 2008. The Possible Origin and
1323 Persistence of Life on Enceladus and Detection of Biomarkers in the Plume. Astrobiology 8,
1324 909-919.
- 1325 McKay, C.P. 2016. Titan as the Abode of Life. Life, 6, 8.
- 1326 McKinnon, W.B. 2015. Effect of Enceladus's rapid synchronous spin on interpretation of
1327 Cassini gravity. Geophysical Research Letters 42, 2137-2143.
- 1328 Mitri, G., Showman, A.P. 2005. Convective conductive transitions and sensitivity of a
1329 convecting ice shell to perturbations in heat flux and tidal-heating rate: Implications for
1330 Europa. Icarus 177, 447-460.
- 1331 Mitri, G., Showman, A.P., Lunine, J.I., Lorenz, R.D. 2007. Hydrocarbon lakes on Titan.
1332 Icarus 186, 385-394.

- 1333 Mitri, G., Bland, M.T., Showman, A.P., Radebaugh, J., Stiles, B., Lopes, R.M.C., Lunine,
1334 J.I., Pappalardo, R.T. 2010. Mountains on Titan: Modeling and observations. *Journal of*
1335 *Geophysical Research (Planets)* 115, E10002.
- 1336 Mitri, G., Meriggiola, R., Hayes, A., Lefevre, A., Tobie, G., Genova, A., Lunine, J.I., Zebker,
1337 H. 2014a. Shape, topography, gravity anomalies and tidal deformation of Titan. *Icarus* 236,
1338 169-177.
- 1339 Mitri, G., and 16 colleagues 2014b. The exploration of Titan with an orbiter and a lake probe.
1340 *Planetary and Space Science* 104, 78-92.
- 1341 Moore, J.M., Howard, A.D. 2010. Are the basins of Titan's Hotei Regio and Tui Regio sites
1342 of former low latitude seas?. *Geophysical Research Letters* 37, L22205.
- 1343 Mousis, O., Gautier, D., Bockelée-Morvan, D. 2002. An Evolutionary Turbulent Model of
1344 Saturn's Subnebula: Implications for the Origin of the Atmosphere of Titan. *Icarus* 156, 162-
1345 175.
- 1346 Mousis, O., Schmitt, B. 2008. Sequestration of Ethane in the Cryovolcanic Subsurface of
1347 Titan. *The Astrophysical Journal* 677, L67.
- 1348 Mousis, O., and 10 colleagues 2009. Clathration of Volatiles in the Solar Nebula and
1349 Implications for the Origin of Titan's Atmosphere. *The Astrophysical Journal* 691, 1780-
1350 1786.
- 1351 Mousis, O., Lunine, J.I., Picaud, S., Cordier, D., Waite, J.H., Jr., Mandt, K.E. 2011. Removal
1352 of Titan's Atmospheric Noble Gases by Their Sequestration in Surface Clathrates. *The*
1353 *Astrophysical Journal* 740, L9.
- 1354 Neish, C.D., Somogyi, A., Smith, M.A. 2010. Titan's Primordial Soup: Formation of Amino
1355 Acids via Low-Temperature Hydrolysis of Tholins. *Astrobiology* 10, 337-347.
- 1356 Neish, C.D., Lorenz, R.D. 2012. Titan's global crater population: A new assessment.
1357 *Planetary and Space Science* 60, 26-33.
- 1358 Neish, C.D., and 14 colleagues 2015. Spectral properties of Titan's impact craters imply
1359 chemical weathering of its surface. *Geophysical Research Letters* 42, 3746-3754.
- 1360 Neish, C.D., Molaro, J.L., Lora, J.M., Howard, A.D., Kirk, R.L., Schenk, P., Bray, V.J.,
1361 Lorenz, R.D. 2016. Fluvial erosion as a mechanism for crater modification on Titan. *Icarus*
1362 270, 114-129.
- 1363 Niemann, H.B., and 17 colleagues 2005. The abundances of constituents of Titan's
1364 atmosphere from the GCMS instrument on the Huygens probe. *Nature* 438, 779-784.
- 1365 Niemann, H.B., Atreya, S.K., Demick, J.E., Gautier, D., Haberman, J.A., Harpold, D.N.,
1366 Kasprzak, W.T., Lunine, J.I., Owen, T.C., Raulin, F. 2010. Composition of Titan's lower
1367 atmosphere and simple surface volatiles as measured by the Cassini-Huygens probe gas

- 1368 chromatograph mass spectrometer experiment. *Journal of Geophysical Research (Planets)*
1369 115, E12006.
- 1370 Nimmo, F., Pappalardo, R.T. 2016. Ocean worlds in the outer solar system, *J. Geophys. Res.*,
1371 in press.
- 1372 Nixon, C.A., and 12 colleagues 2012. Isotopic Ratios in Titan's Methane: Measurements and
1373 Modeling. *The Astrophysical Journal* 749, 159.
- 1374 O'Brien, D.P., Lorenz, R.D., Lunine, J.I. 2005. Numerical calculations of the longevity of
1375 impact oases on Titan. *Icarus* 173, 243-253.
- 1376 Owen, T., Niemann, H.B. 2009. The origin of Titan's atmosphere: some recent advances.
1377 *Philosophical Transactions of the Royal Society of London Series A* 367, 607-615.
- 1378 Pollock, R., Haring, R.E., Holden, J.R., Johnson, D.L., Kapitanoff, A., Mohlman, D., Phillips,
1379 C., Randall, D., Rechsteiner, D., Rivera, J. and Rodriguez, J.I., 2010, October. The Orbiting
1380 Carbon Observatory instrument: performance of the OCO instrument and plans for the OCO-2
1381 instrument. In *Remote Sensing* (pp. 78260W-78260W). International Society for Optics and
1382 Photonics.
- 1383 Porco, C.C., and 24 colleagues 2006. Cassini Observes the Active South Pole of Enceladus.
1384 *Science* 311, 1393-1401.
- 1385 Porco, C., DiNino, D., Nimmo, F. 2014. How the Geysers, Tidal Stresses, and Thermal
1386 Emission across the South Polar Terrain of Enceladus are Related. *The Astronomical Journal*
1387 148, 45.
- 1388 Postberg, F., Kempf, S., Hillier, J.K., Srama, R., Green, S.F., McBride, N., Grun, E. 2008.
1389 The E-ring in the vicinity of Enceladus. II. Probing the moon's interior. The composition of
1390 E-ring particles. *Icarus* 193, 438-454.
- 1391 Postberg, F., Kempf, S., Schmidt, J., Brilliantov, N., Beinsen, A., Abel, B., Buck, U., Srama,
1392 R. 2009. Sodium salts in E-ring ice grains from an ocean below the surface of Enceladus.
1393 *Nature* 459, 1098-1101.
- 1394 Postberg, F., Schmidt, J., Hillier, J., Kempf, S., Srama, R. 2011. A salt-water reservoir as the
1395 source of a compositionally stratified plume on Enceladus. *Nature* 474, 620-622.
- 1396 Postberg, F., Khawaja, N., Hsu, H.W., Sekine, Y., Shibuya, T. 2015. Refractory Organic
1397 Compounds in Enceladus' Ice Grains and Hydrothermal Activity. AGU Fall Meeting
1398 Abstracts.
- 1399 Radebaugh, J., Lorenz, R.D., Kirk, R.L., Lunine, J.I., Stofan, E.R., Lopes, R.M.C., Wall,
1400 S.D., the Cassini Radar Team 2007. Mountains on Titan observed by Cassini Radar. *Icarus*
1401 192, 77-91.

- 1402 Radebaugh, J., and 15 colleagues 2008. Dunes on Titan observed by Cassini Radar. *Icarus*
1403 194, 690-703.
- 1404 Radebaugh, J., Lorenz, R., Farr, T., Paillou, P., Savage, C., Spencer, C. 2010. Linear dunes
1405 on Titan and earth: Initial remote sensing comparisons. *Geomorphology* 121, 122-132.
- 1406 Rappaport, N.J., Iess, L., Wahr, J., Lunine, J.I., Armstrong, J.W., Asmar, S.W., Tortora, P.,
1407 Di Benedetto, M., Racioppa, P., 2008. Can Cassini detect a subsurface ocean in Titan from
1408 gravity measurements? *Icarus* 194, 711–720.
- 1409 Raulin, F. 2008. Organic lakes on Titan. *Nature* 454, 587-589.
- 1410 Rauscher, B.J., Figer, D.F., Regan, M.W., Boeker, T., Garnett, J., Hill, R.J., Bagnasco, G.,
1411 Balleza, J., Barney, R., Bergeron, L.E. and Brambora, C., 2004, October. Detectors for the
1412 James Webb Space Telescope near-infrared spectrograph. In *SPIE Astronomical Telescopes+*
1413 *Instrumentation* (pp. 710-726). International Society for Optics and Photonics.
- 1414 Rauscher, B.J., Lindler, D.J., Mott, D.B., Wen, Y., Ferruit, P. and Sirianni, M., 2011. The
1415 Dark Current and Hot Pixel Percentage of James Webb Space Telescope 5 μ m Cutoff
1416 HgCdTe Detector Arrays as Functions of Temperature. *Publications of the Astronomical*
1417 *Society of the Pacific*, 123(906), p.953.
- 1418 Reh, K., Spilker, L., Lunine, J.I., Waite, J.H., Cable, M.L., Postberg, F. and Clark, K., 2016,
1419 March. Enceladus Life Finder: The search for life in a habitable Moon. In *Aerospace*
1420 *Conference, 2016 IEEE* (pp. 1-8)
- 1421 Rieke, M.J., Kelly, D. and Horner, S., 2005, August. Overview of James Webb Space
1422 Telescope and NIRCams Role. In *Optics & Photonics 2005* (pp. 590401-590401).
1423 International Society for Optics and Photonics.
- 1424 Roth, L., Saur, J., Retherford, K.D., Strobel, D.F., Feldman, P.D., McGrath, M.A., Nimmo, F.
1425 2014. Transient Water Vapor at Europa's South Pole. *Science* 343, 171-174.
- 1426 Scherer, S., K. Altwegg, H. Balsiger, J. Fischer, A. Jäckel, A. Korth, M. Mildner, D. Piazza,
1427 H. Rème, and P. Wurz, A novel principle for an ion mirror design in time-of-flight mass
1428 spectrometry, *Int. Jou. Mass Spectr.* 251 (2006) 73–81.
- 1429 Schinder, P.J. et al. 2015. A numerical technique for two-way radio occultations by oblate
1430 axisymmetric atmospheres with zonal winds. *Radio Science* 50 (7), pp. 712-727.
- 1431 Schinder, P.J. et al. 2012. The structure of Titan's atmosphere from Cassini radio occultations:
1432 Occultations from the Prime and Equinox missions. *Icarus*, 221, 1020-1031.
- 1433 Schläppi, B., and 12 colleagues 2010. Influence of spacecraft outgassing on the exploration of
1434 tenuous atmospheres with in situ mass spectrometry. *Journal of Geophysical Research (Space*
1435 *Physics)* 115, A12313.

- 1436 Schmidt, J., Brilliantov, N., Spahn, F., Kempf, S. 2008. Slow dust in Enceladus' plume from
1437 condensation and wall collisions in tiger stripe fractures. *Nature* 451, 685-688.
- 1438 Schubert, G., Anderson, J.D., Travis, B.J., Palguta, J. 2007. Enceladus: Present internal
1439 structure and differentiation by early and long-term radiogenic heating. *Icarus* 188, 345-355.
- 1440 Senft, L.E., Stewart, S.T. 2011. Modeling the morphological diversity of impact craters on
1441 icy satellites. *Icarus* 214, 67-81.
- 1442 Sherwood L., B., Westgate, T.D., Ward, J.A., Slater, G.F., Lacrampe-Couloume, G. 2002.
1443 Abiogenic formation of alkanes in the Earth's crust as a minor source for global hydrocarbon
1444 reservoirs. *Nature* 416, 522-524.
- 1445 Soderblom, J.M., Bell, J.F., Johnson, J.R., Joseph, J. and Wolff, M.J., 2008. Mars Exploration
1446 Rover Navigation Camera in-flight calibration. *Journal of Geophysical Research: Planets*,
1447 113(E6).
- 1448 Soderblom, J.M., Brown, R.H., Soderblom, L.A., Barnes, J.W., Jaumann, R., Le Mouélic, S.,
1449 Sotin, C., Stephan, K., Baines, K.H. and Buratti, B.J., Clark, R.N., Nicholson, P.D., 2010.
1450 Geology of the Selk crater region on Titan from Cassini VIMS observations. *Icarus*, 208(2),
1451 pp.905-912.
- 1452 Soderblom, J.M., Barnes, J.W., Soderblom, L.A., Brown, R.H., Griffith, C.A., Nicholson,
1453 P.D., Stephan, K., Jaumann, R., Sotin, C., Baines, K.H. and Buratti, B.J., 2012. Modeling
1454 specular reflections from hydrocarbon lakes on Titan. *Icarus*, 220(2), pp.744-751.
- 1455 Soderblom, L.A., Becker, T.L., Kieffer, S.W., Brown, R.H., Hansen, C.J., Johnson, T.V.,
1456 Kirk, R.L., Shoemaker, E.M., Cook, A.F. 1990. Triton's geyser-like plumes - Discovery and
1457 basic characterization. *Science* 250, 410-415.
- 1458 Soderblom, L.A., and 26 colleagues 2007. Correlations between Cassini VIMS spectra and
1459 RADAR SAR images: Implications for Titan's surface composition and the character of the
1460 Huygens Probe Landing Site. *Planetary and Space Science* 55, 2025-2036.
- 1461 Solomonidou, A., Hirtzig, M., Coustenis, A., Bratsolis, E., Le Mouélic, S., Rodriguez, S.,
1462 Stephan, K., Drossart, P., Sotin, C., Jaumann, R., Brown, R.H., Kyriakopoulos, K., Lopes,
1463 R.M.C., Bampasidis, G., Stamatelopoulou-Seymour, K., Moussas, X. (2014). Surface albedo
1464 spectral properties of geologically interesting areas on Titan. *J. of Geophys. Res.*, 119, 1729-
1465 1747.
- 1466 Solomonidou, A., A. Coustenis, M. Hirtzig, S. Rodriguez, K. Stephan, R.M.C. Lopes, P/
1467 Drossart, C. Sotin, S. Le Mouélic, K. Lawrence, E. Bratsolis, R. Jaumann and R.H. Brown,
1468 (2016). Temporal variations of Titan's surface with Cassini/VIMS, *Icarus* 270, 85-99.
- 1469 Sotin, C. et al., 2005. Release of volatiles from a possible cryovolcano from near-infrared
1470 imaging of Titan. *Nature*, 435, 786-798.

- 1471 Spahn, F., and 15 colleagues 2006. Cassini Dust Measurements at Enceladus and Implications
1472 for the Origin of the E Ring. *Science* 311, 1416-1418.
- 1473 Sparks, W. B., Hand, K. P., McGrath, M. A., Bergeron, E., Cracraft, M., and Deustua, S. E.,
1474 2016. Probing for Evidence of Plumes on Europa with HST/STIS. *Ap. J.* 829:121. Sparks,
1475 W.B., Schmidt, McGrath, M. A., Hand, K. P., Spencer, J. R., Cracraft, M., and Deustua, S. E.,
1476 2017. Active Cryovolcanism on Europa?, *Ap. J. Lett.*, 839:L18.
- 1477 Srama, R., and 17 colleagues 2015. Enceladus Icy Jet Analyzer (ENIJA): Search for life with
1478 a high resolution TOF-MS for in situ characterization of high dust density regions. *European*
1479 *Planetary Science Congress 2015*, EPSC2015-769.
- 1480 Stevens, T.O., McKinley, J.P. 1995. Lithoautotrophic Microbia, Ecosystems in Deep Basalt
1481 Aquifers. *Science* 270, 450-454.
- 1482 Stofan, E.R., and 37 colleagues 2007. The lakes of Titan. *Nature* 445, 61-64.
- 1483 Stofan, E., Lorenz, R., Lunine, J., Bierhaus, E., Clark, B., Mahaffy, P., and Ravine, M.,
1484 TiME—The Titan Mare Explorer, *IEEE Aerospace Conference*, IEEE Publ., Piscataway, NJ,
1485 March 2013, pp. 1–10.
- 1486 Strange, N., Spilker, T., Landau, D., Lam, T., Lyons, D. and Guzman, J., 2009. Mission
1487 Design for the Titan Saturn System Mission Concept. *Advances in the Astronautical*
1488 *Sciences*, 135(2), pp.919-934.
- 1489 Tobie, G., Teanby, N.A., Coustenis, A., Jaumann, R., Raulin, F., Schmidt, J., Carrasco, N.,
1490 Coates, A.J., Cordier, D., De Kok, R. and Geppert, W.D., 2014. Science goals and mission
1491 concept for the future exploration of Titan and Enceladus. *Planetary and Space Science*, 104,
1492 pp.59-77.
- 1493 Thomas, P.C., Tajeddine, R., Tiscareno, M.S., Burns, J.A., Joseph, J., Loredó, T.J.,
1494 Helfenstein, P., Porco, C. 2016. Enceladus's measured physical libration requires a global
1495 subsurface ocean. *Icarus* 264, 37-47.
- 1496 Thompson, W.R., Sagan, C. 1992. Organic chemistry on Titan: Surface interactions.
1497 *Symposium on Titan* 338.
- 1498 Tobie, G., Grasset, O., Lunine, J.I., Mocquet, A., Sotin, C. 2005. Titan's internal structure
1499 inferred from a coupled thermal-orbital model. *Icarus* 175, 496-502.
- 1500 Tobie, G., Lunine, J.I., Sotin, C. 2006. Episodic outgassing as the origin of atmospheric
1501 methane on Titan. *Nature* 440, 61-64.
- 1502 Tobie, G., Gautier, D., Hersant, F. 2012. Titan's Bulk Composition Constrained by Cassini-
1503 Huygens: Implication for Internal Outgassing. *The Astrophysical Journal* 752, 125.
- 1504 Tobie, G., Lunine, J. I., Monteux, J., Mousis, O., Nimmo, F. 2013. The origin and evolution
1505 of Titan. *Titan: Interior, Surface, Atmosphere and Space Environment*, 24-55.

- 1506 Tomasko, M.G., and 39 colleagues 2005. Rain, winds and haze during the Huygens probe's
1507 descent to Titan's surface. *Nature* 438, 765-778.
- 1508 Turtle, E.P., and 13 colleagues 2011. Rapid and Extensive Surface Changes Near Titan's
1509 Equator: Evidence of April Showers. *Science* 331, 1414.
- 1510 Vuitton, V., Yelle, R.V., McEwan, M.J. 2007. Ion chemistry and N-containing molecules in
1511 Titan's upper atmosphere. *Icarus* 191, 722-742.
- 1512 Yelle, R.V., Cui, J., Müller-Wodarg, I.C.F. 2008. Methane escape from Titan's atmosphere.
1513 *Journal of Geophysical Research (Planets)* 113, E10003.
- 1514 Yung, Y.L., Allen, M., Pinto, J.P. 1984. Photochemistry of the atmosphere of Titan -
1515 Comparison between model and observations. *The Astrophysical Journal Supplement Series*
1516 55, 465-506.
- 1517 Waite, J.H., and 13 colleagues 2006. Cassini Ion and Neutral Mass Spectrometer: Enceladus
1518 Plume Composition and Structure. *Science* 311, 1419-1422.
- 1519 Waite, J.H., Young, D.T., Cravens, T.E., Coates, A.J., Crary, F.J., Magee, B., Westlake, J.
1520 2007. The Process of Tholin Formation in Titan's Upper Atmosphere. *Science* 316, 870.
- 1521 Waite, J.H., Jr., and 15 colleagues 2009. Liquid water on Enceladus from observations of
1522 ammonia and ⁴⁰Ar in the plume. *Nature* 460, 487-490.
- 1523 Waite, J. H. et al. 2006. Cassini ion and neutral mass spectrometer: Enceladus plume
1524 composition and structure. *Science*, 311(5766), 1419-1422.
- 1525 Waite, J.H., and 12 colleagues 2017. Cassini finds molecular hydrogen in the Enceladus
1526 plume: Evidence for hydrothermal processes. *Science*, 356 (6334), 155-159.
- 1527 Wiederschein, F., Vöhringer-Martinez, E., Postberg, F. et al. 2015. Charge Separation and
1528 Isolation in Strong Water Droplet Impacts, *Phys. Chem. Chem. Phys.*, Vol 17, p. 6858-6864,
1529 DOI: 10.1039/C4CP05618C.
- 1530 Wilson, E.H., Atreya, S.K. 2009. Titan's Carbon Budget and the Case of the Missing Ethane.
1531 *Journal of Physical Chemistry A* 113, 11221-11226.
- 1532 Wurz, P., Abplanalp, D., Tulej, M., Lammer, H. 2012. A neutral gas mass spectrometer for
1533 the investigation of lunar volatiles. *Planetary and Space Science* 74, 264-269.
- 1534 Wurz, P., and 18 colleagues 2015. Solar wind sputtering of dust on the surface of 67P
1535 Churyumov-Gerasimenko. *Astronomy and Astrophysics* 583, A22.
- 1536 Zahnle, K., Pollack, J.B., Grinspoon, D., Dones, L. 1992. Impact-generated atmospheres over
1537 Titan, Ganymede, and Callisto. *Icarus* 95, 1-23.
- 1538 Zahnle, K.J., Korycansky, D.G., Nixon, C.A. 2014. Transient climate effects of large impacts
1539 on Titan. *Icarus* 229, 378-391.

1540 TABLES AND FIGURES

1541

1542 **Table 1** E.²T Science Goals and Objectives.

Science Goals	Science Objectives
Origin and evolution of volatile-rich ocean worlds, Enceladus and Titan	<ul style="list-style-type: none">• Are Enceladus' volatile compounds primordial or have they been re-processed and if so, to what extent?• What is the history and extent of volatile exchange on Titan?• How has Titan's organic-rich surface evolved?
Habitability and potential for life of ocean worlds, Enceladus and Titan	<ul style="list-style-type: none">• Is Enceladus' aqueous interior an environment favourable to the emergence of life?• To what level of complexity has prebiotic chemistry evolved in the Titan system?

1543

1544

1545 **Table 2.** Summary of Instrument Characteristics.

Instrument/ Experiment (Proposed Agency)	Mass (kg)	Peak Power (W)	TRL	Science Contribution
INMS (SSO)	6.2	34	6	1) Analysis of elemental, molecular and isotopic composition of neutral and ionic gas phase constituents in a mass range of 1–1000 u/e in Saturn’s E-ring, Enceladus’ plume and Titan’s upper atmosphere 2) Search for spatial variations in composition and correlate with jet sources.
ENIJA (DLR)	6.5	19.2	5–6	1) Analysis of elemental, molecular and isotopic composition of solid phase constituents in a mass range of 1–2000 u of Enceladus’ plume / E-ring 2) Measure fluxes at high impact rates up to 108 s-1m-2 to map the dynamical profile (number density, ejection speeds and size distribution) of Enceladus’ ice jets
TIGER (NASA)	45	30	5–6	1) Detailed analysis of the geology of Titan’s surface at 30–100 m/pixel and of Enceladus’ plume sources at 1 m/pixel 2) Measure of the thermal emission from Enceladus’s south polar terrain, at 1 m/pixel
Total	57.7	83.2		

1546

1547

1548

1549 **Table 3.** Nominal interplanetary trajectory

Departure	
Launch date to GTO	April 2030
Hyperbolic Injection date	27 April 2030
Injection ΔV from upper stage (km/s)	1.20
Injected Mass (kg)	4056
C_3 (km ² /s ²)	9.58
Declination of escape asymptote (deg)	5
Cruise	
Earth flyby date	20 August 2031
Earth flyby altitude (km)	500
Earth flyby V-infinity (km/s)	9.28
S/C mass at Earth flyby	3637
Arrival	
Saturn arrival date	26 April 2036
Flight time (years)	6.0
Arrival V-infinity (km/s)	5.72
Arrival declination (deg)	19.0
SOI ΔV (m/s)	569
Range at SOI (R_S)	1.05
Orbital period (day)	150
Apoapsis range (R_S)	180
S/C mass after SOI (kg)	2753

1550

1551

1552 **Table 4.** Launch period performance, fixed arrival date.

Launch Date	Nominal -10 days	Nominal (27Apr2030)	Nominal+10days
C ₃ (km ² /s ²)	9.58	9.58	9.58
Xe propellant (kg)	750	747	752
SOI ΔV (m/s)	563	569	571

1553

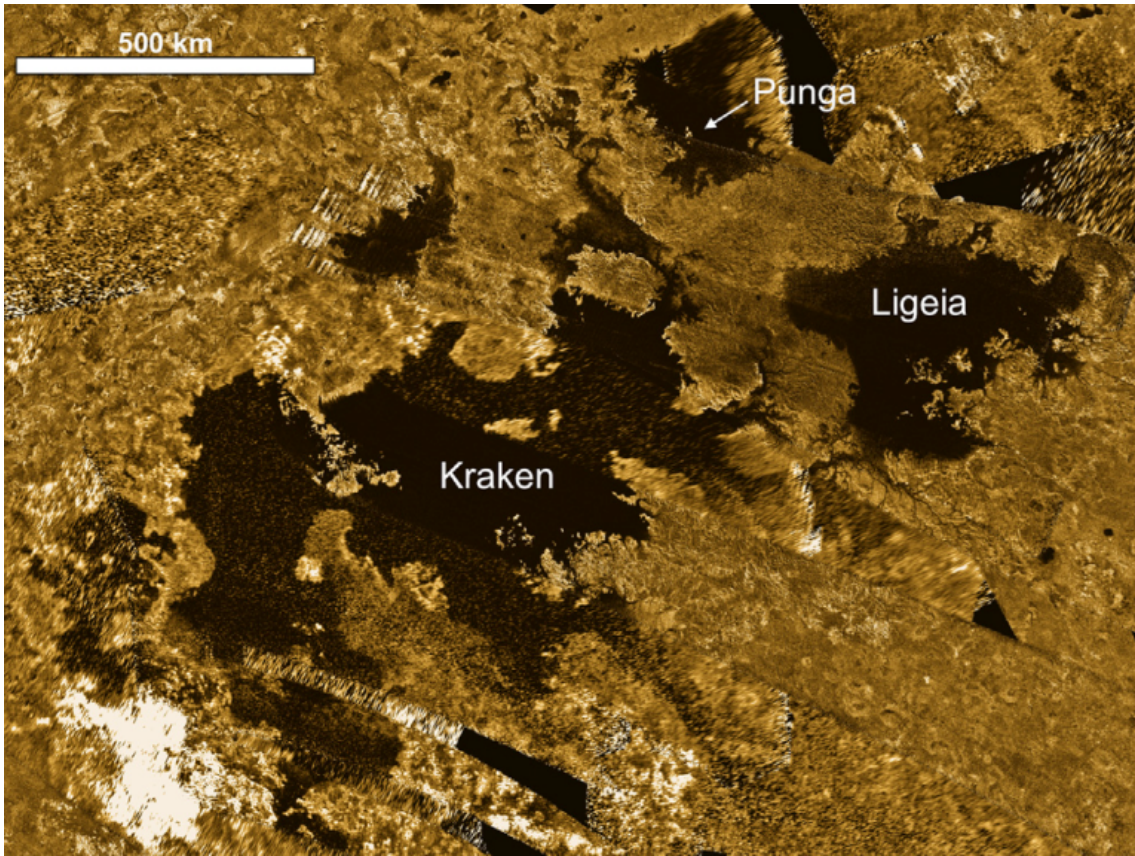
1554

1555 **Table 5.** E²T spacecraft technical characteristics.

E²T Spacecraft main technical characteristics		Heritage
Spacecraft Dimensions	<ul style="list-style-type: none"> Main S/C body: 2974mm × 2860mm × 2589mm with 4 Solar Array wings of an overall area of 160 m². SEPS cylindrical section: 600mm radius × 970mm height with 3+1 QinetiQ T6-Ion Thruster Engine of 7.5 kW each one. 	ExoMars BepiColombo
Overall Launch mass	<ul style="list-style-type: none"> 4056 kg (including 58 kg of science payload), dry mass 1876 kg 	
Propulsion Architecture	<p>The E²T S/C propulsion architecture is based on the integration of three different propulsion systems:</p> <ul style="list-style-type: none"> Solar Electrical Propulsion System (SEPS) based on 3+1 QinetiQ T6 gridded Ion-Thruster engines (1 for redundancy) Main Bi-propellant propulsion system for S/C manoeuvres purposes Hydrazine Mono-propellant propulsion system of 16 RCS Thruster (8+8 in hot redundancy) for Attitude and Orbital Control System (AOCS) purposes. 	ExoMars BepiColombo
Power Architecture	<p>The E²T Electrical Propulsion System (EPS) architecture proposed is based on:</p> <ul style="list-style-type: none"> 4 Solar Array Wings able to sustain an End of Life (EOL) power demand of 620 W (including margins) with a reference solar constant of 15 W/m² at 9.14 AU, with a Sun-Aspect-Angle of 0°. One 31 kg Li-Ion battery of 3691 Wh total capacity and able to sustain a peak power load of demand of 700 W during the forecast eclipses. One secondary battery installed on SEPS module for 100 V High-Voltage Sun-regulated power bus stability purposes. 	JUICE Rosetta BepiColombo
Baseline payload	<ul style="list-style-type: none"> Ion and Neutral Mass Spectrometer (INMS) Enceladus Icy Jet Analyser (ENIJA) Titan Imaging and Geology, Enceladus Reconnaissance (TIGER) high-resolution infrared camera 	

1556

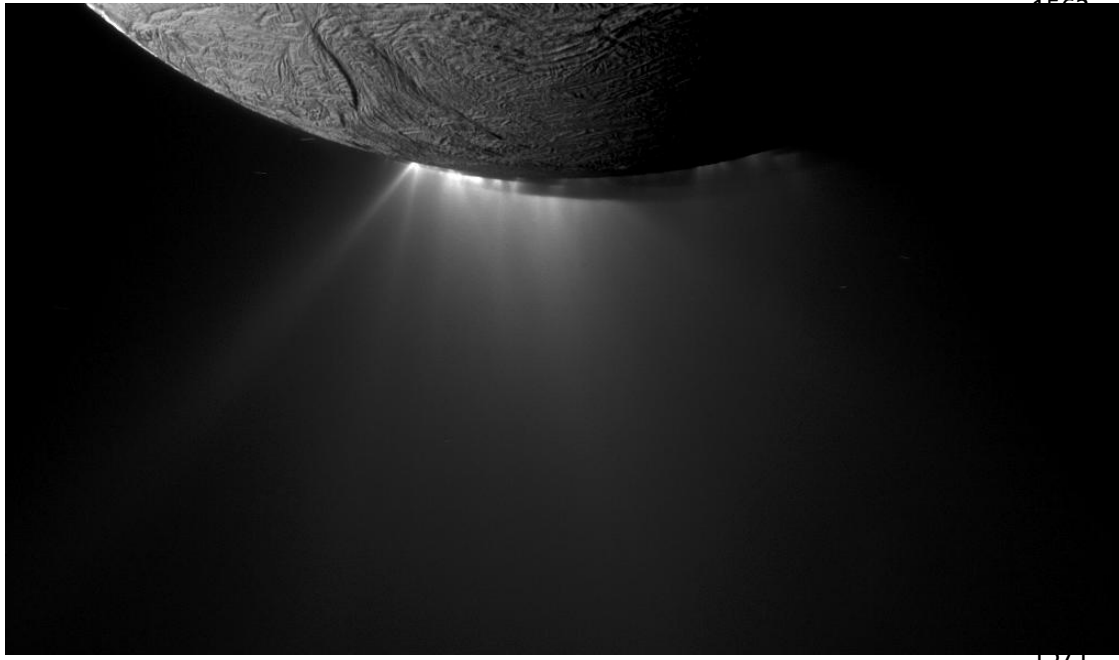
1557



1558

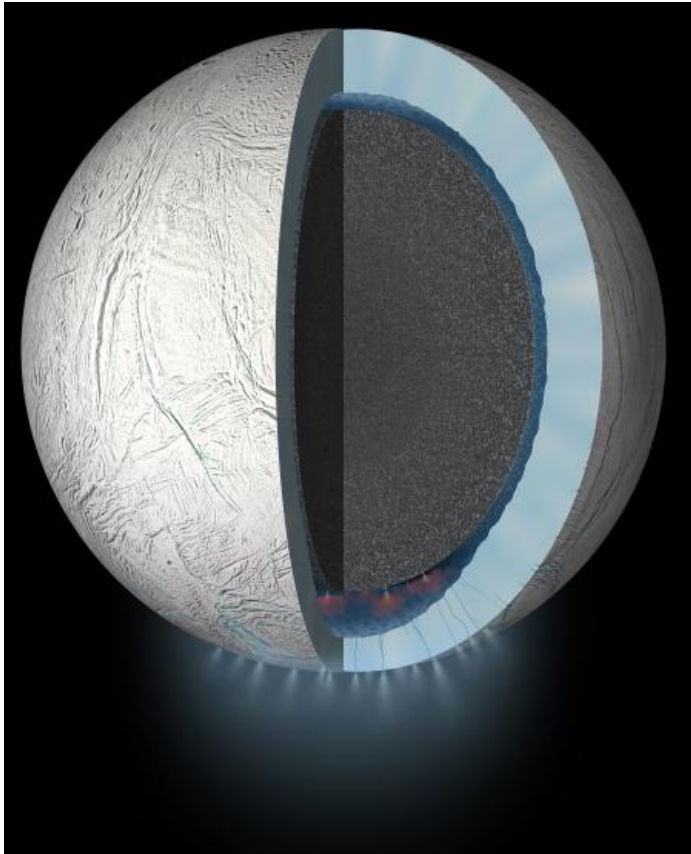
1559 **Figure 1.** Cassini SAR mosaic images of the north polar region showing Kraken, Ligeia and Punga
1560 Maria (from Mitri et al., 2014a).

1561



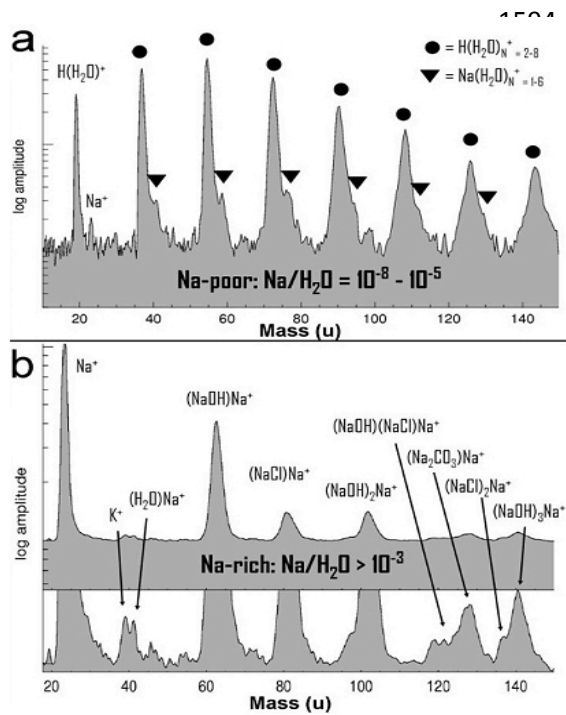
1572 **Figure 2.** Plume emanating from multiple jets in Enceladus' south polar terrain
1573 (NASA/JPL/Space Science Institute).

1574



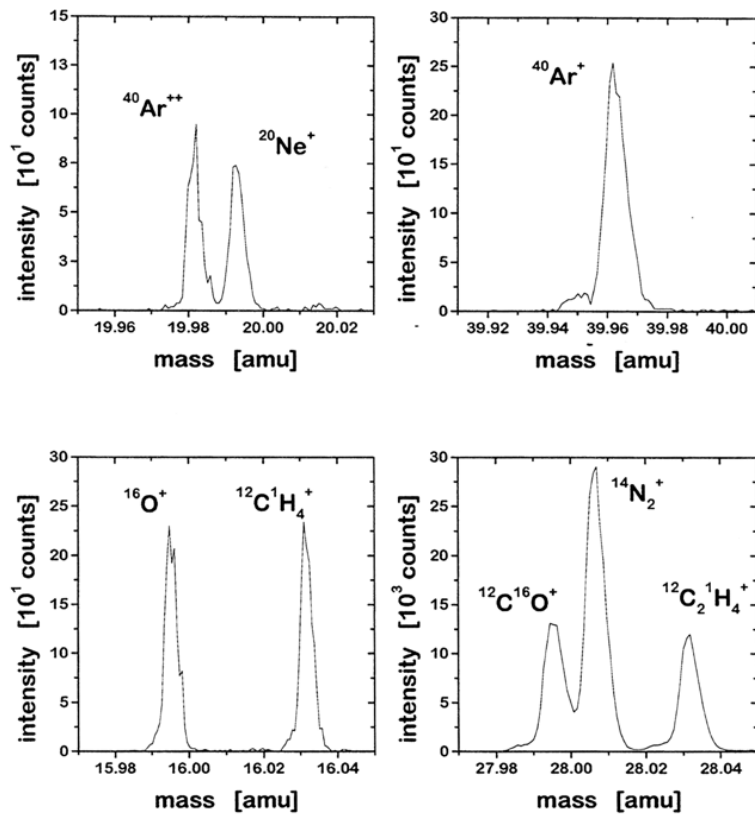
1588 **Figure 3.** Enceladus' internal structure inferred from gravity, topography and libration
1589 measurement provided by Cassini mission. A global subsurface ocean is present under the
1590 outer ice shell. The ice shell is believed to be a few kilometers thin at the south polar region
1591 where the center of the geological activity is with the formation of the plume formed by
1592 multi-jets (NASA/JPL-Caltech).

1593



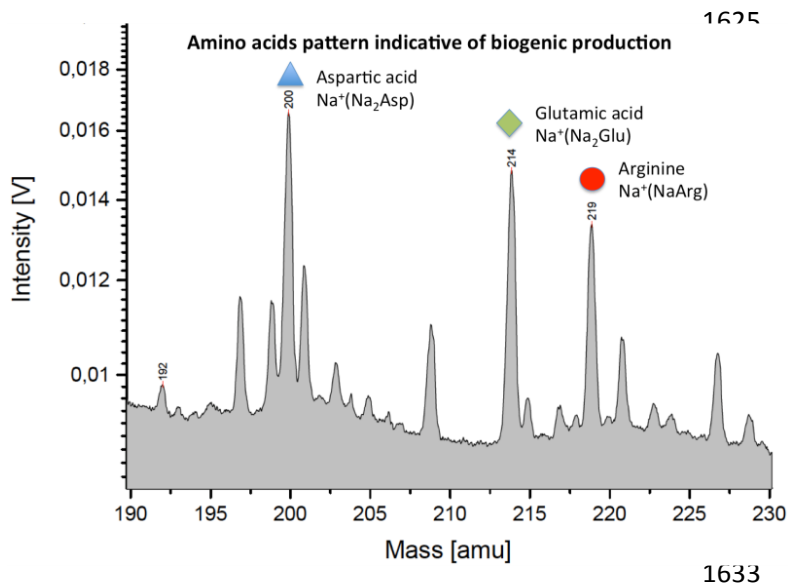
1605 **Figure 4.** Composition of salt-poor (Type I and II) and salt-rich (Type III) particles in
 1606 Saturn's E-ring and Enceladus' plume as measured by Cassini CDA instrument (Postberg et
 1607 al., 2009).

1608



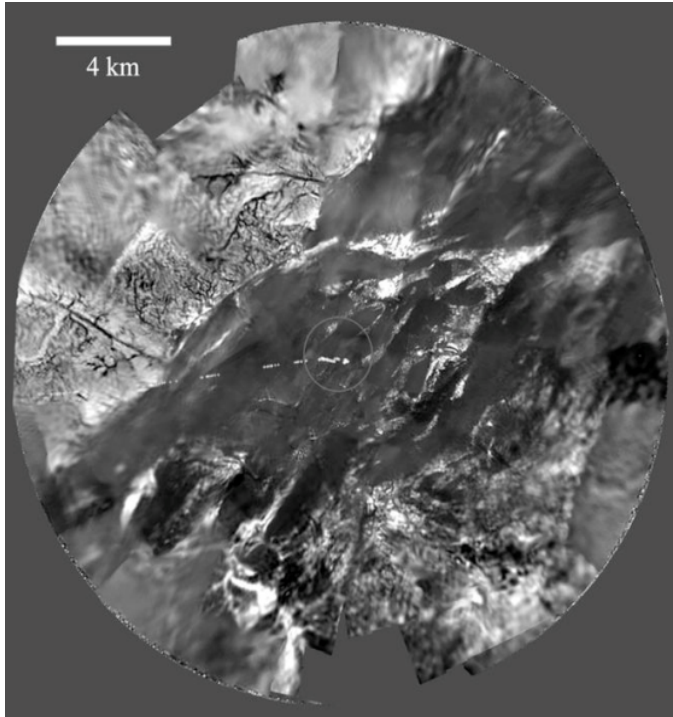
1621 **Figure 5.** Separation of isobaric interference such as occur at 16, 20, 28, and 40 u/e for the
 1622 indicated species is possible based on heritage of RTOF/ROSINA from the Rosetta mission
 1623 (Scherer et al., 2006; Wurz et al., 2015).

1624



1634 **Figure 6.** Laser dispersion mass spectrum of aspartic acid (12 ppm), glutamic acid (12 ppm),
 1635 and arginine (8 ppm) dissolved in a salt-water matrix simulating Enceladus' ocean
 1636 composition. The complex amino acids are detectable in comparable quantities to glycine (15
 1637 ppm, not shown), even though the spectrum has a mass resolution 3 times less than ENIJA's.
 1638 S/N ratio of this laser dispersion spectrum is comparable to a much lower analysed
 1639 concentration in ENIJA spectra (≤ 1 ppm). Most un-annotated mass lines are due to salt-water
 1640 cluster ions. By co-adding multiple ice grain spectra the S/N ratio can be further improved
 1641 leading to an ENIJA detection limit of 10–100 ppb for most amino acids in ice grains formed
 1642 from Enceladus' ocean water.

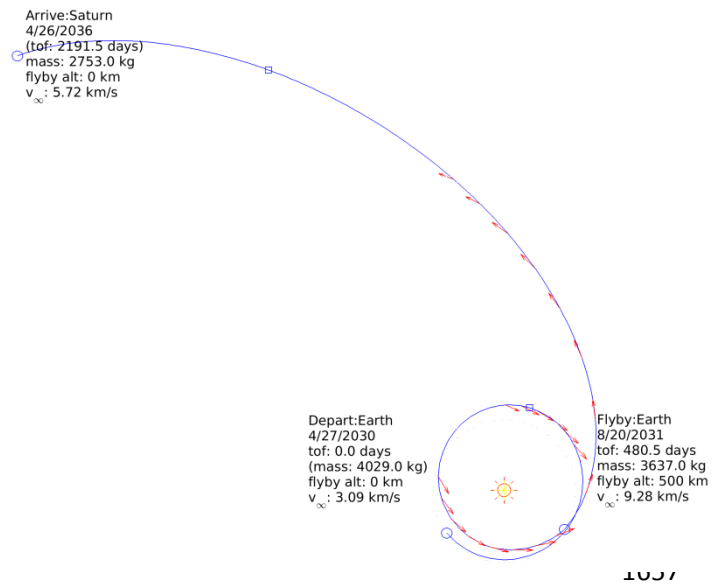
1643



1644

1645 **Figure 7.** The surface of Titan imaged by DISR camera during the Huygens probe descend.
1646 TIGER has the capability to image Titan at Huygens DISR resolution
1647 (ESA/NASA/JPL/University of Arizona).

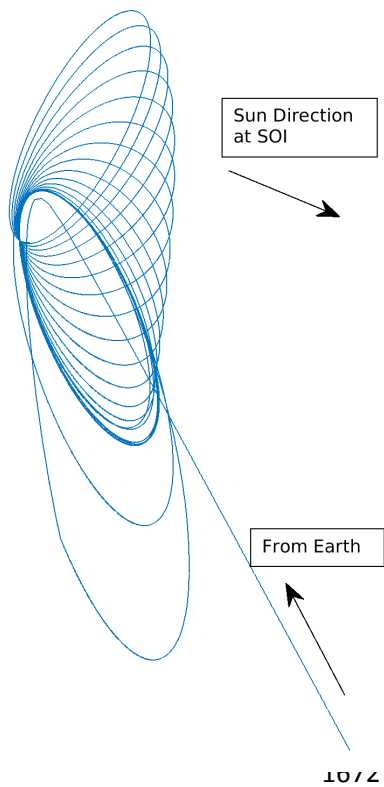
1648



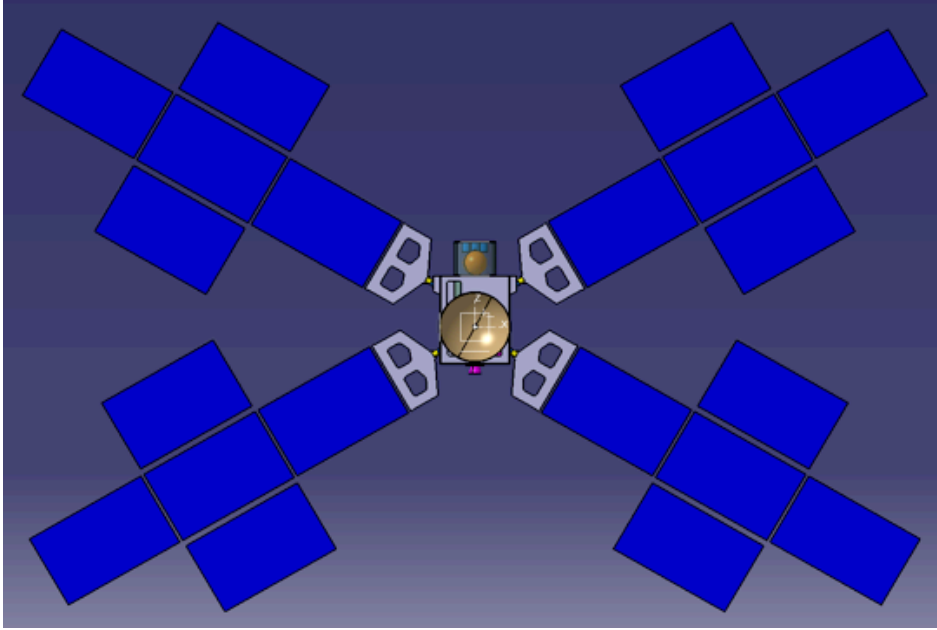
1658 **Figure 8.** Interplanetary transfer to Saturn. Red arrows indicate electric propulsion thrust.

1659

1660



1673 **Figure 9.** Sample tour with two period- and inclination-management Titan flybys followed
 1674 by a science phase with 6 Enceladus flybys and 17 Titan flybys (Inertial representation).
 1675



1676

1677 **Figure 10.** E²T baseline proposed configuration of the S/C.

1678